

Article

Modeling the Optimal Transition of an Urban Neighborhood towards an Energy Community and a Positive Energy District

Diego Viesi ^{1,*}, Gregorio Borelli ^{1,2}, Silvia Ricciuti ¹, Giovanni Pernigotto ² and Md Shahriar Mahbub ^{1,3}

¹ Center for Sustainable Energy, Fondazione Bruno Kessler (FBK), Via Sommarive 18, 38123 Trento, Italy; gregorio.borelli@student.unibz.it (G.B.); sricciuti@fbk.eu (S.R.); shaikatcse@gmail.com (M.S.M.)

² Faculty of Engineering, Free University of Bozen-Bolzano (UNIBZ), Piazza Università 5, 39100 Bolzano, Italy; giovanni.pernigotto@unibz.it

³ Department of Computer Science and Engineering, Ahsanullah Univeristy of Science & Technology (AUST), Love Road 141&142, Tejgaon Industrial Area, Dhaka 1208, Bangladesh

* Correspondence: viesi@fbk.eu

Abstract: Building renovation is a key initiative to promote energy efficiency, the integration of renewable energy sources (RESs), and a reduction in CO₂ emissions. Supporting these goals, emerging research is dedicated to energy communities and positive energy districts. In this work, an urban neighborhood of six buildings in Trento (Italy) is considered. Firstly, the six buildings are modeled with the Urban Modeling Interface tool to evaluate the energy performances in 2024 and 2050, also accounting for the different climatic conditions for these two time periods. Energy demands for space heating, domestic hot water, space cooling, electricity, and transport are computed. Then, EnergyPLAN coupled with a multi-objective evolutionary algorithm is used to investigate 12 different energy decarbonization scenarios in 2024 and 2050 based on different boundaries for RESs, energy storage, hydrogen, energy system integration, and energy community incentives. Two conflicting objectives are considered: cost and CO₂ emission reductions. The results show, on the one hand, the key role of sector coupling technologies such as heat pumps and electric vehicles in exploiting local renewables and, on the other hand, the higher costs in introducing both electricity storage to approach complete decarbonization and hydrogen as an alternative strategy in the electricity, thermal, and transport sectors. As an example of the quantitative valuable finding of this work, in scenario S1 “all sectors and EC incentive” for the year 2024, a large reduction of 55% of CO₂ emissions with a modest increase of 11% of the total annual cost is identified along the Pareto front.

Keywords: urban modeling interface; EnergyPLAN; multi-objective evolutionary algorithm; energy community; positive energy district



check for updates

Citation: Viesi, D.; Borelli, G.; Ricciuti, S.; Pernigotto, G.; Mahbub, M.S.

Modeling the Optimal Transition of an Urban Neighborhood towards an Energy Community and a Positive Energy District. *Energies* **2024**, *17*, 4047. <https://doi.org/10.3390/en17164047>

Academic Editors: Fabrizio Reale and Teresa Castiglione

Received: 8 July 2024

Revised: 5 August 2024

Accepted: 9 August 2024

Published: 15 August 2024



Copyright: © 2024 by the authors. Licensee MDPI, Basel, Switzerland. This article is an open access article distributed under the terms and conditions of the Creative Commons Attribution (CC BY) license (<https://creativecommons.org/licenses/by/4.0/>).

1. Introduction

Global warming and climate change represent persistent challenges confronting the global community. A wealth of scientific inquiry has conclusively established a discernible connection between these challenges and the escalating anthropogenic emissions, particularly the mounting concentration of greenhouse gasses (GHGs).

Considering these challenges, concerted international endeavors have been undertaken to mitigate GHG emissions. The Kyoto Protocol, a landmark international agreement, was established in 1997 [1]. Subsequently, the Paris Agreement emerged as a pivotal development during the 21st United Nations Climate Change Conference (COP21) in 2015 [2]. To meet the stipulated targets delineated in the Paris Agreement, the European Commission embraced the Green Deal in 2019 [3]. This visionary framework outlines an extensive array of policies and strategies, charting a course towards achieving a sustainable and carbon-neutral economy by the year 2050.

Amidst the various sectors implicated in these transformative initiatives, the building sector emerges as particularly pivotal. Responsible for a substantial 36% of GHG emissions

and constituting a significant 40% of the overall energy consumption, the building sector assumes a central role in the pursuit of climate goals [4]. To align with the stringent mandates of the European Climate Law, by 2030 the European Union must reduce buildings' greenhouse gas emissions by 60%, their energy consumption by 14%, and the energy consumption of heating and cooling by 18% [4]. However, the current reality presents a stark contrast, with a meager 0.2% of the annual renovations in Europe meeting the stringent criteria for the deep renovation necessary to achieve these benchmarks [4]. In a bid to address this pressing issue, a comprehensive strategy has been championed in 2020—the Renovation Wave Strategy [4]. This strategic approach aspires to double the annual rate of deep renovations by the year 2030, thereby ushering in a transformative wave of sustainable building practices and contributing significantly to the overarching goals of emission reduction and environmental sustainability.

Alongside the European Commission policy action, emerging research is dedicated to positive energy districts (PEDs) which are “energy-efficient and energy-flexible urban areas which produce net zero greenhouse gas emissions and actively manage an annual local or regional surplus production of renewable energy” [5]. PEDs can exploit local energy communities to promote renewable energy source (RES) sharing and the integration of different energy systems and infrastructures. Some cities have adopted such PED-related developments and, to support such initiatives, European countries have collaborated to achieve 100 PEDs by 2025 through a comprehensive research and innovation program (JPI Urban Europe PED program) [6]. JPI Urban Europe has collected information on energy transition and sustainable urbanization projects across Europe; the 61 collected cases are summarized in a PED Booklet [7], including the Santa Chiara Urban District in Trento (Italy) that is also the specific case study of this paper. The Santa Chiara Urban District, composed of six buildings, is also one of the three demo sites of the Horizon Europe InCUBE project [8]. InCUBE envisions to “unlock the EU renovation wave through cutting-edge standardised and integrated processes based on industrialisation, innovative renewable energy technologies, digitalisation, and new market entrants” [8]. Among the new market entrants, novel business models include the formation of Renewable Energy Communities (RECs).

This paper discusses the coupling of two different software, the Urban Modeling Interface 3.0 (umi) for dynamic building energy modeling, defining the hourly profiles of electricity, space heating, domestic hot water (DHW), and space cooling demands in different climate conditions, and EnergyPLAN + MOEA as an optimization model to explore the energy, cost, and CO₂ emission performance of multiple dynamic and integrated energy systems. The district hourly transport demand is considered based on the parking spaces pertaining to each building and it is included in the EnergyPLAN + MOEA modeling.

With respect to building energy performance assessment, the common building energy modeling (BEM) approach is not a feasible solution due to the large amount of input data required for characterization and the high computational cost when applied at the district level. For these reasons, urban building energy modeling (UBEM) has recently been developed to extend the capabilities of BEM to model the energy consumption of large groups of buildings and to evaluate issues related to the interactions and interdependencies between buildings and economies of scale [9,10]. There are a number of tools for modeling urban environments in the literature, reported, for example, by Battini et al. (2023) [11]. Among them, the Urban Modeling Interface 3.0 (umi), developed in 2012 by the Sustainable Design Lab (Massachusetts Institute of Technology, Cambridge, MA, USA), presents an efficient approach based on the definition of thermal “shoeboxes” that models the energy performance of buildings while maintaining sufficient accuracy and reducing simulation time [12].

EnergyPLAN [13], developed at Aalborg University (DK), is one of the simulators based on the smart energy system concept. This concept was introduced by Lund et al. [14] and integrates the electricity, thermal, and transport sectors, developing new forms of

flexibility [15] and improving RES integration [16]. The combination of large solution space, high temporal resolution, and smart energy systems means that finding the optimal solution is computationally challenging and energy system models are important for developing energy transition pathways and determining their impacts. EnergyPLAN has the capability to integrate with other models as summarized in Table 1.

Table 1. Literature review of the coupling of EnergyPLAN with other tools. The abbreviations used are as follows: DH = district heating; EV = electric vehicle; HP = heat pump; MED = Mediterranean; PV = photovoltaic; RE = renewable energy; V2G = vehicle-to-grid.

Reference	Combined Tool	Type of Case Study
Bhuvanesh et al. [17]	LEAP	The development of a plan for electricity generation expansion, aiming for low carbon emissions in the future. A case study of Tamil Nadu (India).
Cantarero [18]	LEAP	The Nicaraguan energy system is modeled to review renewable energy policies.
Kiwan and Al-Gharibeh [19]	LEAP, SAM	A 100% renewable electricity supply scenario is constructed and compared with three other scenarios. A case study of Jordan.
Matak et al. [20]	LEAP	The possibility of the integration of a combined heat and power waste incineration plant into the existing gas-based district heating system in the central European city. A case study of the City of Zagreb (Croatia).
Campos et al. [21]	LEAP	The compatibility of wind and solar energy resources with the projections of future electricity demand in Hungary. A case study of Hungary.
Dominkovic et al. [22]	MATLAB	Analyze how district cooling systems in hot and humid climates are beneficial solutions, especially in future energy systems, dominated by large shares of intermittent renewable energy sources. A case study of Singapore.
Bamisile et al. [23]	MATLAB	A dynamic analysis of vehicle-to-grid, batteries, and hydro storage for optimal RE integration. A case study of China.
Bamisile et al. [24]	MATLAB	Electrification and renewable energy's future interdependence. An overarching analysis of hydrogen production and electric vehicles integrality in renewable energy penetration. A case study of developing countries.
Doepfert and Castro [25]	MATLAB	Optimized 100% renewable energy system for countries with high shares of hydropower. A case study of Portugal.
Tomic et al. [26]	MATLAB	The influence of legislation changes on the new incineration plants. Case studies of Zagreb (Croatia) and Sønderborg (Denmark).
Pupo-Roncillo et al. [27]	MATLAB	The role of energy storage and cross-border interconnections in increasing the flexibility of future power systems. A case study of Colombia.
Pastore et al. [28]	MATLAB	Improving Italian energy strategy by means of smart energy system approach. A case study of Italy.
Cabrera et al. [29]	MATLAB	A description of the MATLAB Toolbox for EnergyPLAN (MaT4EnergyPLAN), a set of functions developed to manage the EnergyPLAN software using MATLAB. A case study of Denmark.
De Luca et al. [30]	TRNSYS	The economic and energy feasibility analysis of a renewable energy system for a small city to convert it to zero greenhouse gas city by 2030. A case study of Altavilla Silentina (Italy).
Bonati et al. [31]	TRNSYS	The integration of exergy criterion in energy planning analysis for 100% renewable system. A case study of Pompeii (Italy).
Calise et al. [32]	TRNSYS	A novel paradigm for mobility sectors related to shopping centers based on PV panels and EVs. A case study of Campania (Italy).
Battaglia et al. [33]	TRNSYS, DesignBuilder	An integrated energy plan for Campania satisfying the European and Italian targets of reducing CO ₂ emissions by 2050. A case study of Campania (Italy).
Novosel et al. [34]	MATSim	Model the hourly distribution of the energy consumption of EVs and use the calculated load curves to test their impact. A case study of Croatia.

Table 1. Cont.

Reference	Combined Tool	Type of Case Study
Thellufsen et al. [35]	Markal/TIMES	EnergyPLAN and Markal/TIMES combined enable a better analysis of heating scenarios. Potential for the implementation of district heating in a future energy system originally intended not to include district heating. A case study of Ireland.
Groppi et al. [36]	Homer	An economically optimized smart energy system in a small MED island is designed. A case study of Favignana Island (Italy).
Østergaard et al. [37]	energyPRO	Comparing straw boilers and heat pump district heating systems. A case study of Samsø (Denmark).
Pfeifer et al. [38]	MultiNode	The integration of renewable energy and demand response technologies (i.e., V2G) in interconnected energy systems. Case studies of Vis, Korcula, Lastovo, and Mljet (Croatia).
Bačeković and Østergaard [39]	MultiNode	Firstly, a 100% local renewable energy system is created based on the interplay between the electricity, heating, and transport sectors. Secondly, an analysis of the integration of the proposed local system with the rest of the country is carried out. A case study of Varaždin County (Croatia).
Lund et al. [40]	Modest	Assess the economic potential for introducing HPs in DH in Denmark. A case study of Denmark.
Pillai et al. [41]	DIgSILENT PowerFactory	The comparison of hourly and dynamic power balancing models for validating future energy scenarios. A case study of Bornholm (Denmark).
Jiménez et al. [42]	PowerWorld, MATLAB	The integration of renewable energy sources in islanded energy systems, focusing on the electrification of the transport sector. The method combines an overall energy system analysis with more detailed power system analyses. A case study of Gran Canaria (Spain).
Olkkonen et al. [43]	Tailored demand-side response model	Assess demand shifting in the residential and commercial sectors and how those affect the hourly operation of the Finnish energy system, taking into account both the electricity and district heating sectors. A case study of Finland.

In 2016, Mahbub et al. [44] developed the coupling of a multi-objective evolutionary algorithm (MOEA) and EnergyPLAN to find optimal energy scenarios. Since then, there have been a significant number of case studies using the same or similar scheme. The case studies range from the national scale (e.g., Italy by Prina et al. [45] and Bellocchi et al. [46], Croatia by Herc et al. [47], and India by Laha and Chakraborty [48]) to the regional scale (e.g., in Italy, the Province of Trento by Viesi et al. [49], the Region of Valle d'Aosta by Bellocchi et al. [50], and the Province of South Tyrol by both Prina et al. [51] and Vaccaro and Rocco [52], and in Austria, the Region of Niederösterreich by Prina et al. [53]), valleys (e.g., Val di Non [54] and Giudicarie Esteriori [55] in Italy by Mahbub et al. [55]), islands (Lanzarote in Spain by Cabrera et al. [56] and Favignana in Italy according to Groppi et al. [57]), and local scales (e.g., Aalborg Municipality in Denmark by Yuan et al. [58], Bressanone-Brixen in Italy by Prina et al. [59]), including industrial sites (such as the Italian refinery Sonatrach by de Maigret et al. [60]).

In 2023, Viesi et al. [61] addressed the optimized modeling of an energy community at the valley scale. Specifically, an effort has been carried out by an Italian energy cooperative, called CEIS, to design decarbonization energy scenarios for the years 2030 and 2050, the latter considering the full decarbonization target. The CEIS case study is set in a mountain area composed of five municipalities with very small villages (249 km² and 8372 inhabitants). Concerning energy demands, taking into account only the availability of real monitoring data for electricity consumption, the thermal consumption of the buildings was calculated with simple formulas that consider statistical data relating to the number of buildings, their surface area, age, type of construction, renovation rate, and type of heat generator. Transport consumption, on the other hand, takes into account statistics on the number of vehicles, type of fuel, and average km traveled.

Therefore, from the study of the existing literature, it appears to the authors of this paper that the innovative contribution lies in the integration of EnergyPLAN with both detailed umi modeling and MOEA to find optimal energy scenarios for an urban neighborhood both in the current (2024) and in the future (2050) climate, considering the PED and energy community approaches.

The remainder of the paper is organized as follows: in Section 2, the materials and methods are described; in Section 3, the results are presented and discussed; in Section 4, conclusive remarks are provided.

2. Materials and Methods

The research follows a three-step methodology (Figure 1). The initial phase involves collecting and analyzing building information specific to the district and the characterization of climate conditions. These pieces of information, coupled with standard parameters, are the input for the second phase based on the UBEM of the district, developed in umi. The UBEM allows one to characterize the (hourly) district energy needs which are the inputs to the EnergyPLAN + MOEA model. The district transport demand is also considered based on the parking spaces pertaining to each building and evaluating the annual and hourly demand of energy for the mobility of each parking space (corresponding to a car, considering the same assumptions of the study for the Province of Trento by Viesi et al. [49]). Finally, in EnergyPLAN + MOEA, multiple configurations of energy systems are assessed to evaluate energy community incentives, costs, and CO₂ emissions.

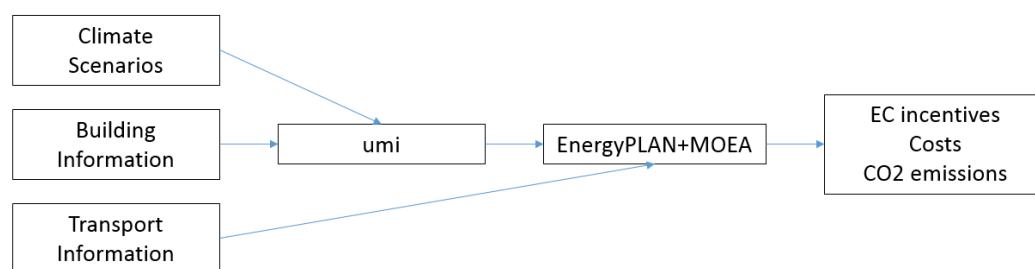


Figure 1. Study workflow.

2.1. Case Study

The Santa Chiara district in Trento (Figure 2) is one of the three demo sites of the Horizon Europe project called InCUBE (2022–2026). The project aims to develop the tools and a methodology to accelerate the rate of deep renewal, which is essential for the renovation wave that will sweep the European Union in the coming years to achieve the goal of decarbonization. The project involves 23 partners from 7 different European countries [8].

The Santa Chiara district has been in a status of progressive abandonment since the late nineties of the last century, with social marginality and building decay, a lack of space protection, and crime episodes (theft, mugging, and harassment). It is composed of (I) 5 publicly owned buildings (B1, B2, B3, B4, and B6, to be renovated) for tertiary uses and residential spaces, (II) a mixed-use, residential–tertiary, private complex consisting of two buildings (B5 to be built by Habitat S.p.a.), and (III) a large green space. In 2016, the Municipality of Trento drew the “Program for re-functionalization and sustainable reuse of the area Santa Chiara”, involving buildings B1 to B5, and the park. The total amount of investment is EUR 41 million and has been recently funded by the Italian Government for EUR 18 million. More recently, the Municipality of Trento has decided to extend the intervention area also to the “Santa Chiara Cultural Services Centre” (B6), securing additional funding of EUR 9 million. InCUBE will mainly focus on B6 for the demonstration of the proposed innovations, while buildings B1 to B5 will enhance the district-level approach favoring the emergence of a Renewable Energy Community.

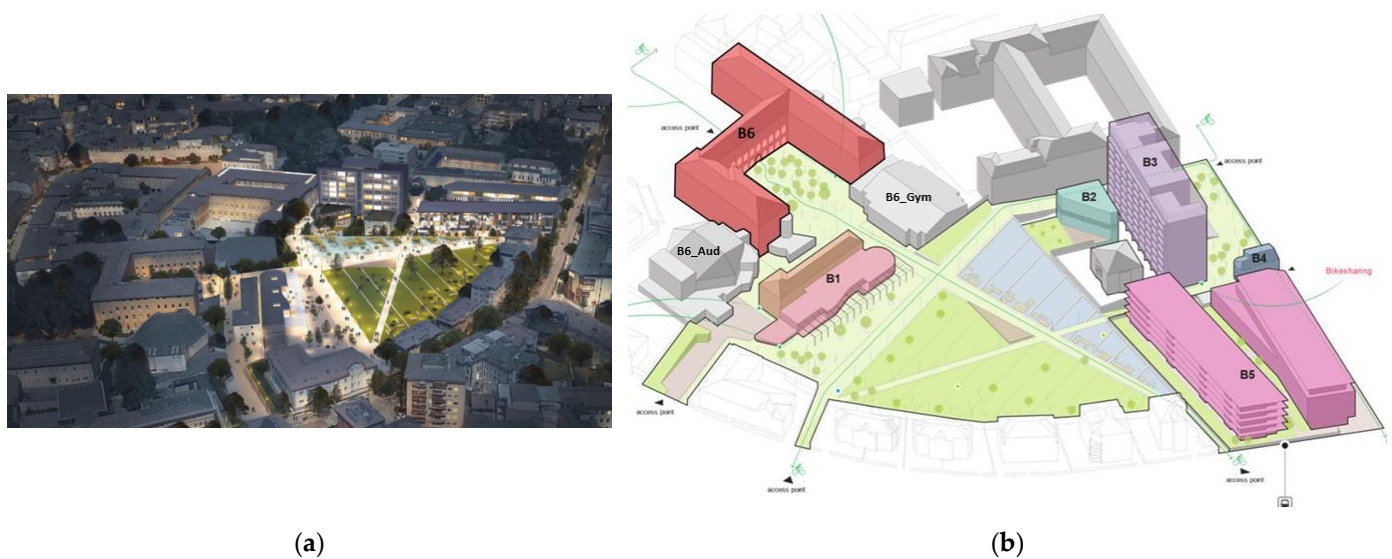


Figure 2. Santa Chiara district: (a) rendering after renovation; (b) buildings involved and IDs.

The main renovation activities in the Santa Chiara district, also involved in the following analysis, are as follows:

- Installing insulation materials, thermal break windows, and LED lighting to decrease building energy consumption.
- Installing photovoltaic panels, solar thermal panels, and heat pumps to increase renewable energy generation.
- Integrating thermal energy storage and batteries to maximize self-consumption.
- Adopting a new low-temperature geothermal district heating and cooling network to maximize the integration of thermal renewable energy at a neighborhood level.
- Installing electric vehicle charging stations to support clean mobility.
- Developing energy management systems for building and district optimization.

Furthermore, in the early stages of the InCUBE project, the Santa Chiara district has been involved in interesting research activities related to (I) the topic of BIM (Building Information Model) to BEM (building energy model) [62] and (II) the topic of dynamic modeling in the programming language Modelica for the energy performance analysis of the renovation process [63].

Figure 2 shows the buildings undergoing renovation and the labels (IDs) used later in the analysis. Building B1 (floor area 1872 m², deep renovation) will be the headquarters of the local Order of Architects and Engineers and an open space, with a co-working area, an event area, and a cafeteria. Building B2 (floor area 796 m², deep renovation) is a day care center for the elderly and a kindergarten, while B4 (floor area 130 m², low renovation) is a former church currently utilized by Cultural Associations. Buildings B3 (floor area 5854 m², deep renovation) and B5 (floor area 7776 m², new building) are the two buildings with the most interventions. B3, which will obtain the net Zero Emission Building (nZEB) label after extensive renovation, will house the municipal technical offices with 270 employees. B5, on the other hand, consists of two new units, one with offices and shops and the other with 68 flats. The Santa Chiara Cultural Services Centre is in building B6 (floor area of this historical part of 5400 m², low renovation), which includes the Cuminetti Theatre, and it is adjacent to the Santa Chiara Auditorium (B6_Aud with an additional floor area of 1607 m², low renovation) and the Palabocchi Gymnasium (B6_Gym with an additional floor area of 1128 m², low renovation). B6 (historical part) will become a multifunctional place with different activities such as the retention of municipal archives, reception, info-points, an exhibition space, administrative spaces, promotion space for incubation and start-up activities, spaces for the Trento Film Festival offices, and the “Cuminetti” experimental theatre, common areas for socializing and recreation and guesthouse areas.

2.2. Climate Scenarios

The district's analysis is assessed under three distinct climate scenarios: two pertaining to the current climate applied both in 2024 and in 2050 and another based on a future climate projection for the year 2050 (Figure 3).

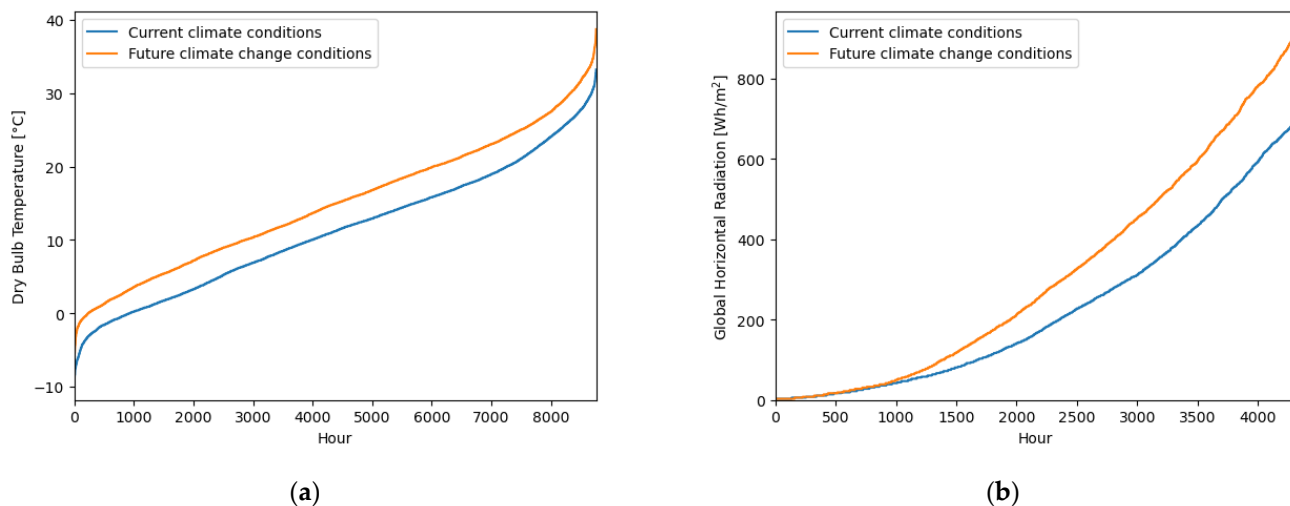


Figure 3. Comparison of current climate conditions (“CS 2024” and “CS 2050 UC”) and future climate change conditions (“CS 2050 ERY_h^I ”) in terms of (a) dry bulb temperature; (b) global horizontal radiation.

The current climate condition is characterized by the standard annual weather conditions provided by the “Comitato Termotecnico Italiano” (CTI) for the Municipality of Trento [64]. These conditions are representative of the anticipated weather patterns for the year 2024, coinciding with the foreseen completion of the district, and of the weather patterns for the year 2050 under the assumption of an unchanged climate (UC).

On the other hand, the second climate profile, known as the extreme reference year with high impact ERY_h^I , is established following the methodology developed by Pernigotto et al. to generate extreme reference years for building energy performance simulation [65]. The climatic year, as for the typical year, is constructed by synthesizing observed data across a period of two decades. Employing statistical tests, the extreme year is discerned by integrating monthly data points exhibiting the most pronounced deviation from the established long-term scenario. Considering that the ERY_h^I signifies a future climate projection with considerable significance and bearing in mind that European benchmarks are predicated on developments up to 2050, the climatic conditions associated with this profile will be referred to as “CS 2050 ERY_h^I ” for all the ensuing future analyses.

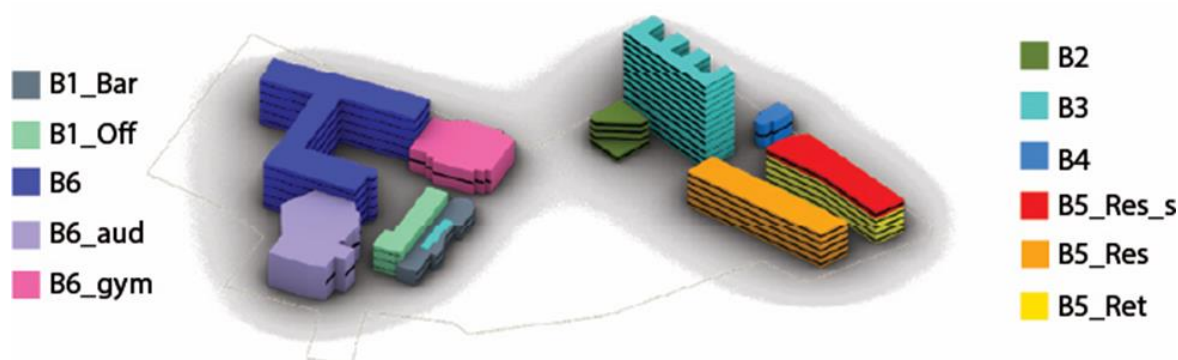
The two climate scenarios, “CS 2024” (same as “CS 2050 UC”) and “CS 2050 ERY_h^I ”, demonstrate substantial variations in key climatic parameters (see Table 2). In “CS 2024”, the average annual temperature is recorded at 11.21 °C, while in “CS 2050 ERY_h^I ”, it rises to 14.92 °C. The Heating Degree Days, with a base temperature of 18 °C (HDD18), experience a decline from 2791 in “CS 2024” to 1852 in “CS 2050 ERY_h^I ”. Conversely, the Cooling Degree Days (CDD18), calculated with the same base temperature of 18 °C, show an opposite trend, increasing from 313 in “CS 2024” to 730 in “CS 2050 ERY_h^I ”. This implies a shift in the climate conditions towards a reduced demand for space heating and an increased demand for space cooling in the future scenario “CS 2050 ERY_h^I ”. Furthermore, the average global horizontal radiation, a measure of the solar radiation received on a horizontal surface, increases from 128 Wh/m² in “CS 2024” to 152.9 Wh/m² in “CS 2050 ERY_h^I ”.

Table 2. Key climatic parameters in the three climate scenarios considered in this study.

	“CS 2024”	“CS 2050 UC”	“CS 2050 ERY _h ¹ ”
Average annual temperature [°C]	11.21	11.21	14.92
HDD18	2791	2791	1852
CDD18	313	313	730
Average global horizontal radiation [°C]	128	128	152.9

2.3. Umi Model

The energy demand of the district is calculated using the umi model (Figure 4). The model considered a total of 6 buildings; however, due to the diverse utilization within some of these buildings and to obtain a more detailed simulation, they were divided into multiple blocks. More specifically, B1 underwent a partitioning into two distinctive blocks: an office block (B1_Off) and a bar zone block (B1_Bar). Similarly, B5 was also subjected to a partitioning approach, resulting in the creation of a retail zone block (B5_Ret) alongside two residential blocks. One of these residential blocks (B5_Res_s) is situated atop the retail area, while the other (B5_Res) forms a separate building within the “Habitat” project. Finally, B6 was separated into three distinct components: B6, B6_Gym (the Palabocchi Gym), and B6_Aud (the Auditorium of Santa Chiara).

**Figure 4.** District umi final model.

The initial step in the process involves creating a 3D model of the buildings using Rhino as the 3D modeling software. Special attention is given to accurately representing the relative distances between buildings to effectively evaluate shading interactions. This is achieved by first creating the building floor plans and then extruding them to their actual heights, resulting in a realistic representation of the buildings.

Since all the data inputs of the buildings (new or deeply renovated) have been taken from their Energy Certificates and Technical Energy Reports, which did not consider detailed modeling of the surrounding urban context, we adopted the same simplified approach for the sake of consistency. Furthermore, the urban morphology of the buildings surrounding the district is similar (in terms of average height) to the analyzed case study. Considering these latter aspects, solar irradiance on the roof (the area considered for PV and thermal panel installation) was not affected by our modeling choice. Finally, Trento is located in a mountain area, where the impact of the urban context is limited compared to the surrounding mountain environment (whose effects are already taken into account in the weather data).

Together with the 3D model of the district, a umi library has to be created to perform the energy simulation. In the library, the building envelope elements, the schedules, and the zone information are defined.

The building envelope is essential for calculating thermal losses and radiation gains, which are fundamental in simulating the energy performance of buildings. Within the umi

library, the building envelope is represented by six elements: external walls, ground, roof, internal partitions, internal slabs, and windows.

The equivalent transmittance is calculated using Equation (1), where U_i and A_i represent the transmittance and the area of element i , respectively.

$$U_{eq} = \frac{\sum U_i A_i}{\sum A_i} \quad (1)$$

The building elements are reconstructed using the most common stratigraphy, and the thickness of the components is adjusted to achieve the desired transmittance values as specified in Table 3. The windows reported in Table 3 are characterized by the following properties:

- Double glazing window: U value of $3.159 \text{ W m}^{-2} \text{ K}^{-1}$ and solar heat gain coefficient equal to 0.601.
- Triple glazing window: U value of $1.507 \text{ W m}^{-2} \text{ K}^{-1}$ and solar heat gain coefficient equal to 0.418.

Table 3. Building characterizations: envelope transmittance, window type, and intended use.

Building ID	External Wall [W m ⁻² K ⁻¹]	Ground Floor [W m ⁻² K ⁻¹]	Roof [W m ⁻² K ⁻¹]	Internal Partitions [W m ⁻² K ⁻¹]	Internal Slab [W m ⁻² K ⁻¹]	Window Type	Intended Use/Schedule Type
B1_Bar	0.22	0.16	0.18	0.53	1.37	Triple Glazing	Community area
B1_Off	0.23	0.54	0.19	0.96	1.30	Triple Glazing	Office
B2	0.21	0.23	0.20	0.70	0.51	Triple Glazing	Community area
B3	0.29	0.54	0.16	0.71	0.20	Triple Glazing	Office
B4	0.70	2.20	0.50	1.60	2.00	Double Glazing	Community area
B5_Ret	0.18	0.80	0.20	0.71	0.20	Triple Glazing	Retail
B5_Res_s	0.11	0.80	0.12	0.56	0.20	Triple Glazing	Residential
B5_Res	0.11	0.80	0.12	0.56	0.20	Triple Glazing	Residential
B6	0.70	2.20	0.50	1.60	2.00	Double Glazing	Community area
B6_Gym	0.70	2.20	0.50	1.60	2.00	Double Glazing	Community area
B6_Aud	0.70	2.20	0.50	1.60	2.00	Double Glazing	Community area

The second stage in the library definition process involves the creation of schedules, which serve as time-dependent representations of the building load and behavior. These schedules cover various components: occupancy, equipment load, DHW usage, mechanical ventilation, and space heating and space cooling set points. The profiles of these components are expressed as values ranging from 0 to 1, with a sensitivity of 0.1. Given that the buildings under consideration are still in the construction phase, the actual schedules and usage data are unavailable. Therefore, to proceed with the simulation, schedule profiles are sourced from authoritative references such as ASHRAE standards [66] and DOE (U.S. Department of Energy) publications [67,68].

The buildings are categorized based on their intended usage into four main categories: residential, retail, office, and community areas. For each building type and schedule, distinct profiles for working days (WDs) and weekends (WEs) are created (Figure 5). Subsequently, the daily profiles are grouped to generate weekly and yearly profiles reflecting the temporal variations in energy demand and occupant behavior over different time spans.

The process of defining thermal zones is achieved through the integration of building envelope and schedule data. The accurate characterization of these zones necessitates the incorporation of critical parameters, such as occupancy loads, equipment loads, DHW demands, internal loads, mechanical ventilation rates, and precise space heating and space cooling set points. The internal loads and the DHW demands are sourced from UNI/TS 11300-1:2014 [69]. Additionally, the mechanical ventilation parameter adheres

to the minimum ventilation rate recommended by the normative UNI 10339:1995 [70], ensuring optimal indoor air quality. The values obtained are reported in Table 4. Please also consider that concerning the average infiltration rates, the following values (where ACH is Air Change per Hour) are applied: 0.35 ACH in the existing historic buildings with a low level of renovation (B4 and B6 with low-quality external windows) and 0.10 ACH in the deeply renovated/new buildings (B1, B2, B3, and B5 with high-quality external windows). Space heating and space cooling set points are chosen according to the standard practice and set equal to 20 °C and 26 °C, respectively.

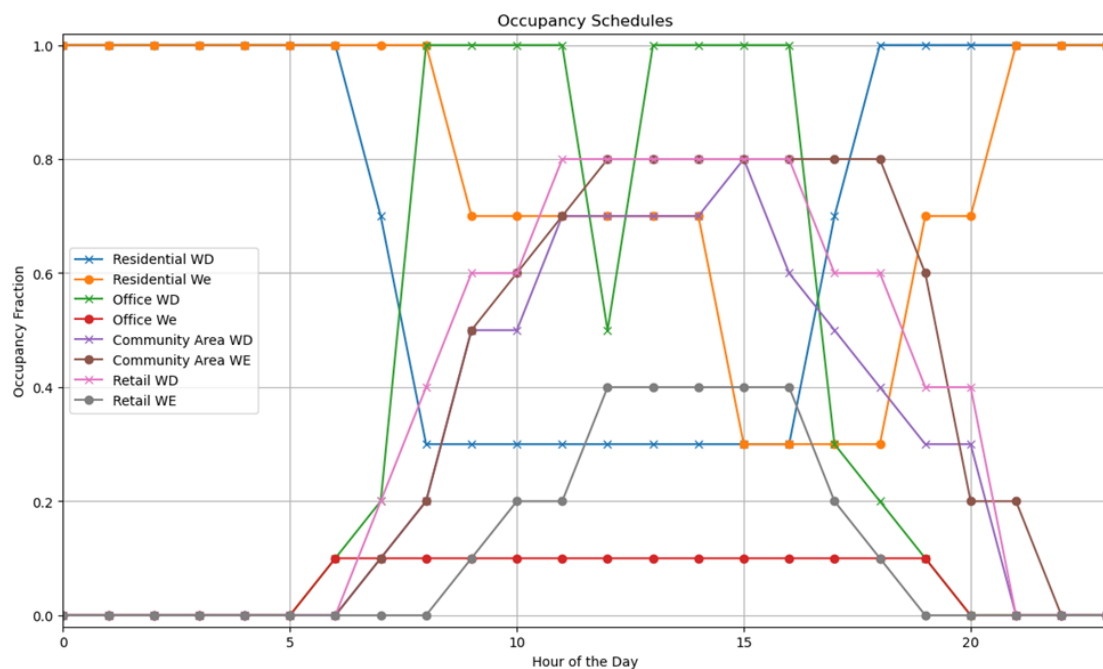


Figure 5. Occupancy profile for a residential building.

Table 4. Zone parameters.

Building ID	Occupancy Density [p m^{-2}]	Internal Loads [W m^{-2}]	Mechanical Ventilation [$\text{m}^3 \text{s}^{-1} \text{p}^{-1}$]	DHW Demand [$\text{m}^3 \text{h}^{-1} \text{m}^{-2}$]
B1_Bar	0.10	10	1.10×10^{-2}	1.16×10^{-4}
B1_Off	0.06	6	1.10×10^{-2}	3.76×10^{-5}
B2	0.10	6	6.00×10^{-3}	2.61×10^{-5}
B3	0.06	6	1.10×10^{-2}	2.42×10^{-4}
B4	1.20	8	6.00×10^{-3}	3.32×10^{-5}
B5_Ret	0.15	8	6.50×10^{-3}	5.92×10^{-5}
B5_Res_s	0.03	4	1.10×10^{-2}	7.36×10^{-5}
B5_Res	0.03	4	1.10×10^{-2}	1.16×10^{-4}
B6	0.10	6	6.00×10^{-3}	2.04×10^{-4}
B6_Gym	0.20	5	6.50×10^{-3}	2.53×10^{-4}
B6_Auditorium	1.50	8	1.25×10^{-2}	1.16×10^{-4}

2.4. EnergyPLAN + MOEA Model

In this section, the process of creating scenarios in EnergyPLAN to assess the environmental and economic impact of the district is outlined. Nineteen technologies are considered as decision variables (Table 5). The heat generators for the case study are the boilers (natural gas and hydrogen), the solar thermal panels, and the heat pumps, the latter can also provide cooling. In local electricity production, the only technology available is photovoltaic (PV). However, the district is connected to the regional electric grid and so can

import electricity from other regional systems; at the same time, the district can also export local excess electricity production. To better exploit local energy production, three types of storage are considered: thermal, battery, and hydrogen. Hydrogen is produced locally in the district via electrolyzers to be used in H2 boilers (in a blending with natural gas from 0 to 100%), FCEV (Fuel Cell Electric Vehicle) or to be stored, including P2P (Power to Power) services. Finally, the transport demand is satisfied by ICEV (Internal Combustion Engine Vehicle), BEV (Battery Electric Vehicle), and FCEV. Overall, in the EnergyPLAN model (I) are considered technologies and energy carriers well known today, (II) particular attention is given to energy efficiency and renewable sources, and (III) of these technologies and energy carriers, the technical, economic, and environmental evolution is analyzed in the 2024–2050 period.

Table 5. The 19 decision variables considered for the Santa Chiara district case study. * thermal demand. The abbreviations used are as follows: BEV = Battery Electric Vehicle; Bl = blending; FCEV = Fuel Cell EV; ICEV = Internal Combustion Engine Vehicle; NG = natural gas; PV = photovoltaic; P2P = Power to Power.

Electrical Sector	Hydrogen Sector	Thermal Sector	Transport Sector
PV (kW)	Bl-Tr Hydrogen Electrolyser (kW)	Solar Thermal * (GWh)	BEV (Mkm)
Battery (kW)	Bl-Tr Hydrogen Storage (MWh)	Heat Pump (heating) * (GWh)	FCEV (Mkm)
Battery (MWh)	P2P Hydrogen Electrolyser (kW)	Heat Pump (cooling) * (GWh)	ICEV (Mkm)
Import (kW)	P2P Hydrogen Fuel Cell (kW)	Boiler NG * (GWh)	
Export (kW)	P2P Hydrogen Storage (MWh)	Boiler Hydrogen * (GWh)	
		Solar Heat Storage (in days of average heat demand)	

Please note that in this study, there is no link between the 2024 scenarios and 2050 scenarios; the two time steps are analyzed completely independently. The aim of the comparison between the two time steps is to see how the scenarios change with the change in climatic conditions and technology parameters (CAPEX, OPEX, lifetime, efficiency, cost of energy carriers, regional/national electricity grid mix, etc.).

Considering the technologies planned in the InCUBE project for the year 2024, Table 6 provides pertinent insights into the allocated power capacities within each building and the total district capacity.

Table 6. Planned installed systems and capacities for the Santa Chiara district case study.

Building ID	Heat Pump Heating [kW]	Heat Pump Cooling [kW]	NG Boiler [kW]	Solar Thermal [kWh/Year]	PV [kW]
B1	136.8	45.9	0	0	24.43
B2	108.63	0	1.39	0	6
B3	304.19	226.4	0	9.62×10^3	20
B4	0	0	25	0	0
B5	145	165	163.2	7.76×10^4	43
B6	0	120	1118	0	77
District	694.62	557.3	1307.59	8.72×10^4	170.43

Additionally, the maximum power installable for PV and solar thermal in both climate conditions (2024 and 2050) has been analyzed considering the available area and the efficiency. With a prudential approach, the available area corresponds to the flat or south-oriented roof area. Please note that for buildings B4 and B6, the installation of PV and solar thermal on their roofs is not possible since they are listed under the Fine Arts Commission. For the PV panels, an efficiency of 20% is assumed for 2024, and improved by 2% in 2050 [49,61]. The annual production of the solar thermal panels for 2024 is calculated as the sum of the hourly power profile (influenced by the optical and thermal efficiency of

the panels, solar radiation, user, and ambient temperature) while for 2050, a technological improvement of 6% is considered [49,61]. Table 7 reports the yield ratios obtained while Table 8 summarizes the maximum technology capacity of each building and of the district.

Table 7. PV and solar thermal yield ratios.

Technology	2024	2050 UC	2050 ERY_h^f
Solar Thermal [kWh/m ²]	478.94	507.67	730.66
PV [m ² /kW _p]	5	4.43	4.43

Table 8. Renewable source maximum capacity.

Building ID	Area [m ²]	2024		2050 UC		2050 ERY_h^f	
		PV [kW]	Solar Thermal [kWh/Year]	PV [kW]	Solar Thermal [kWh/Year]	PV [kW]	Solar Thermal [kWh/Year]
B1	1285.2	257.0	6.16×10^5	289.9	6.54×10^5	289.9	8.84×10^5
B2	220.0	44.0	1.05×10^5	49.6	1.12×10^5	49.6	1.51×10^5
B3	269.9	54.0	1.29×10^5	60.9	1.37×10^5	60.9	1.86×10^5
B4	0.0	0.0	0	0.0	0	0.0	0
B5	2049.0	409.8	9.81×10^5	462.2	1.04×10^6	462.2	1.41×10^6
B6	0.0	0.0	0	0.0	0	0.0	0
B6_gym	482.0	96.4	2.31×10^5	108.7	2.45×10^5	108.7	3.32×10^5
B6_aud	543.0	108.6	2.60×10^5	122.5	2.76×10^5	122.5	3.74×10^5
District	4849.1	989.8	2.32×10^6	1113.8	2.47×10^6	1113.8	3.34×10^6

EnergyPLAN facilitates the comprehensive assessment of the system's total annual cost, encompassing the considerations of both the actualized investment prices and operational expenses. These cost evaluations draw from a pre-existing cost database established through prior studies of the CEIS energy community [61] and Trentino province [49]. Considering the unavailability of the cost data explicitly pertaining to the year 2024, an approach based on linear interpolation is employed to extrapolate the values for this temporal point. The detailed cost values, along with pertinent contextual information, are provided in Supplementary Material A of this study for comprehensive reference.

The adopted simulation scheme is based on the combination of EnergyPLAN and MOEA. EnergyPLAN simulates user-defined scenarios and does not perform the endogenous optimization of the system. Therefore, this software combines well with MOEA, which optimizes output objectives by changing the input decision variables; MOEA is used to solve multi-objective optimization problems when there are several conflicting objectives that must be optimized simultaneously. In addition, MOEA relies on the notion of solution dominance, where a solution is said to be dominant over other solutions if it strictly outperforms them on at least one objective while being non-inferior on all the other objectives. Using this notion of dominance, the set of non-dominated solutions forming the so-called Pareto front can be defined as "optimal solutions".

In the specific case of this study, MOEA is combined with EnergyPLAN, which is able to verify the suitability of the solution (energy system) for the environment. More specifically, EnergyPLAN is used to characterize solutions in terms of CO₂ emissions and total annual costs, and the best solution in each generation is evaluated based on these two parameters. Please note that the total annual cost is calculated by summing three different yearly costs: energy carrier cost (for the purchase of energy carriers), operating cost (or OPEX, to ensure the operation and maintenance of technologies), and investment cost (or CAPEX, for the purchase of technologies, including a 5% interest rate). Each solution is characterized by a certain combination of decision variables (energy technologies) and each decision variable is characterized by several technical, economic, and environmental data (the type of energy carrier used, efficiency, CAPEX, OPEX, lifetime, energy cost, and CO₂

emission factor; see Supplementary Material A). At the end of the process, a Pareto front in the space “CO₂ emissions—total annual costs” is obtained. For more details, see Figure 1 and the description in de Maigret et al. [60].

Table 9 summarizes the MOEA parameters used in this study, which identified 100 optimal energy systems (on the Pareto front) out of 10,000 simulations. The parameter setting of metaheuristic algorithms such as MOEA is experimental. All the parameters in this study are set based on the authors’ experience with the EnergyPLAN + MOEA framework.

Table 9. MOEA parameters used in this work.

MOEA Parameter	Value
Population size	100
Generations	100
Crossover	SBX crossover
Crossover probability	0.9
Mutation	Polynomial mutation
Mutation probability	1/number of decision variables

The analysis of the future optimization scenarios using EnergyPLAN + MOEA is performed by (i) defining the optimization objectives corresponding to the minimization of the total annual costs and CO₂ emissions, and (ii) identifying the decision variables that can be changed within a certain range between the minimum and maximum MOEA boundary values. This study considers 19 decision variables in the electrical, hydrogen, thermal, and transport sectors. In particular, the focus is on cross-sector interconnection and energy storage solutions needed to maximize grid flexibility and the integration of RES.

Overall, this study considers four types of modeling scenarios (Table 10) with different MOEA boundaries, with two time steps corresponding to 2024 and 2050 (the latter under both the ERY_h^I and the assumption of an unchanged climate).

Table 10. Type of scenarios considered for the Santa Chiara district case study.

Type of Scenario	PV and Solar Thermal Constraint	Electricity Demand	Heating Demand	Cooling Demand	Transport Demand	Energy Community Incentive	Only Fossil Fuel Tech vs. H2
S1							
S2							
S3							
S4							

The first type of scenario is called S1 and considers (I) the available roof surfaces for the installation of photovoltaic and solar thermal panels in the district, (II) all the energy demands (electricity, heating, cooling, and transport), and (III) an energy community incentive (assigned to the PV production not exported; therefore, self-consumed by the district, with hourly analysis by EnergyPLAN). The second type of scenario, called S2, corresponds to scenario S1 with the exception of the energy community incentive, which is absent in this case. Moving to S3, this type of scenario is again corresponding to scenario S1 but with the exception of not considering the transport demand. Finally, S4 includes new constraints to explore the hydrogen potential of the district. In fact, this last type of scenario has the same constraints as S1 but with the addition that hydrogen is the only available source for the decarbonization of the heating and transport sectors (through hydrogen boilers and FCEVs, respectively). A further constraint of S4 relates exclusively to electricity storage via hydrogen P2P systems (rather than batteries).

3. Results and Discussion

In this section, the results are presented and analyzed with the same structure as in the methods. First, the umi simulation results are presented. Then, the EnergyPLAN + MOEA scenarios are outlined.

3.1. Umi Results

The umi results are presented for each type of energy demand to better highlight the climate impact on the district.

Concerning the heating demand (HD) (Table 11), composed of space heating (SH) and domestic hot water (DHW), the calculated metrics across the two climate scenarios (2024 and 2050 ERY_h^I) reveal a substantial 28% reduction in the district level, from 2158 MWh/year to 1546 MWh/year. It is noteworthy that the buildings characterized by comparatively lower efficiency, coupled with heightened ventilation rates and infiltration tendencies (B1, B4, and B6), display more pronounced decreases in their heating demands. Moreover, the peak power (PP) consumption profiles also exhibit comprehensive reductions. Please note that DHW consumption is consistent across the climate scenarios, resulting in a final consumption of 324 MWh/year.

Table 11. Heating demand (HD) and peak power (PP) results.

Building ID	HD 2024 and 2050 UC [MWh/Year]	HD 2050 ERY_h^I [MWh/Year]	Δ [%]	PP 2024 and 2050 UC [kW]	PP 2050 ERY_h^I [kW]	Δ [%]
B1	54.84	37.30	−32%	81.45	55.52	−32%
B2	30.77	24.66	−20%	14.46	14.24	−2%
B3	155.43	119.42	−23%	351.81	275.69	−22%
B4	16.40	9.07	−45%	12.46	10.54	−15%
B5	240.79	177.58	−26%	137.61	127.24	−8%
B6	1659.94	1178.00	−29%	1156.44	1101.50	−5%
District	2158.16	1546.03	−28%	1718.85	1375.21	−20%

Moving to the cooling demand (CD) (Table 12), the results indicate a doubling of the district's CD between the two climatic scenarios (from 592 MWh/year in 2024 to 1181 MWh/year in 2050 ERY_h^I), with variations among the buildings. Building B6 experiences a threefold increase, attributed to the substantial ventilation requirements and lower efficiency. Peak power (PP) consumption generally escalates across the buildings, except for a marginal decrease in building B4.

Table 12. Cooling demand (CD) and peak power (PP) results.

Building ID	CD 2024 and 2050 UC [MWh/Year]	CD 2050 ERY_h^I [MWh/Year]	Δ [%]	PP 2024 and 2050 UC [kW]	PP 2050 ERY_h^I [kW]	Δ [%]
B1	40.96	80.29	96%	103.82	117.90	14%
B2	29.16	52.79	81%	67.03	69.28	3%
B3	216.50	363.18	68%	408.55	521.35	71%
B4	13.61	25.04	84%	33.23	28.51	−14%
B5	179.90	320.99	78%	559.37	695.28	24%
B6	111.76	338.66	203%	603.71	962.89	59%
District	591.88	1180.95	100%	1574.38	1949.12	24%

Building B4 is a former small church (130 m² of floor area) to which less interventions on the building envelope are scheduled compared to the other cases in the district (e.g., see Table 3), meaning that larger heat losses are expected in the cooling season with a lower risk of peaks overheating. The explanation for the marginal decrease in cooling PP, however, relies on the weather file construction: as it can be seen in Figure 3, the 2050 ERY_h^I scenario was designed to be hotter but it is still made of actual historical months (the extremes

recorded for Trento). The ERY_h^I weather file is designed to lead to larger space cooling needs, not to maximize the peak load, which can depend on many factors, including the short-term series of temperatures and solar irradiances. Although all the other buildings show also higher cooling peak loads in the 2050 climate change scenario, in the case of B4 (smaller and less insulated), this does not occur and just the cooling need increases, which almost doubles (+84%).

Electricity consumption (not for HP) remains consistent across the climate scenarios, displaying parallel consumption patterns. The annual consumption figures are comprehensively presented in Table 13.

Table 13. Electricity consumption results.

Type of Energy Demand	B1	B2	B3	B4	B5	B6	District
Electricity consumption [MWh/year]	83.73	27.11	222.07	4.95	225.08	401.24	964.16

The comprehensive energy demand, as illustrated in Figure 6, indicates the growing significance of cooling demand from 2024 to 2050 ERY_h^I , reaching levels comparable to the space heating demand. By 2050, space heating, space cooling, and electricity components (other equipment in Figure 6) attain similar significance levels, emphasizing the need for a holistic approach.

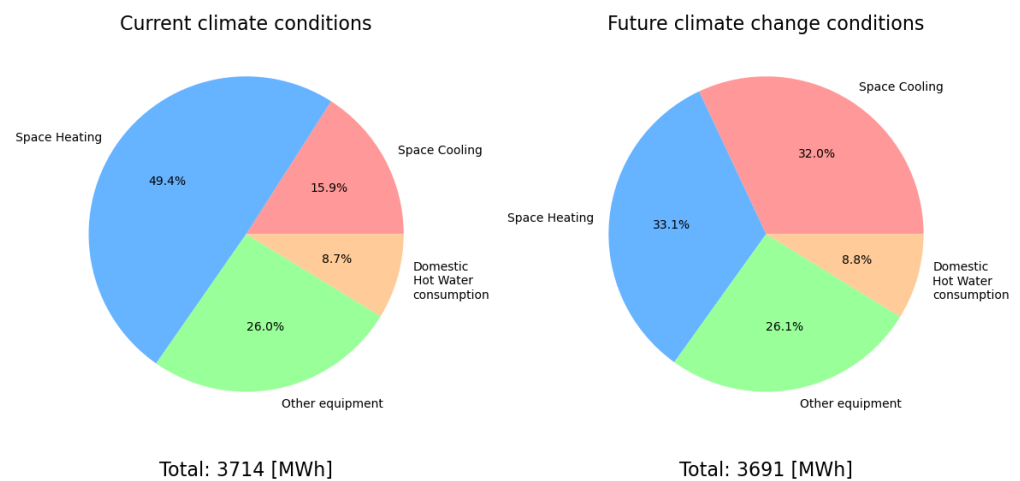


Figure 6. Energy demand partition.

Moreover, Figure 7 demonstrates that in 2024, the heating and cooling demand peaks are comparable, while in 2050, the cooling demand predominantly contributes to the peaks. This observation, coupled with demand shifting, suggests potential variations in electricity demand (for HP) throughout the year, explored in detail within the EnergyPLAN scenarios.

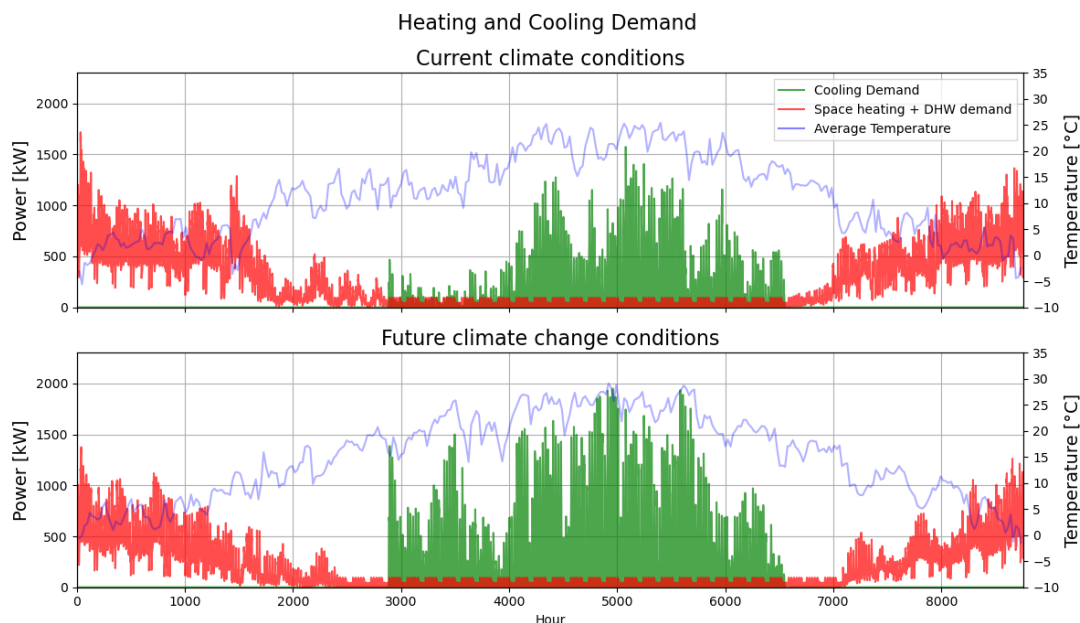


Figure 7. Heating and cooling profile in both climate scenarios.

Figure 8 shows the district umi model with results of the building energy signature simulation for the climate 2024. In red the highest energy demand while in blue the lowest energy demand. Please note that the building energy signature includes all types of energy demand: space heating, domestic hot water, space cooling and electricity components.

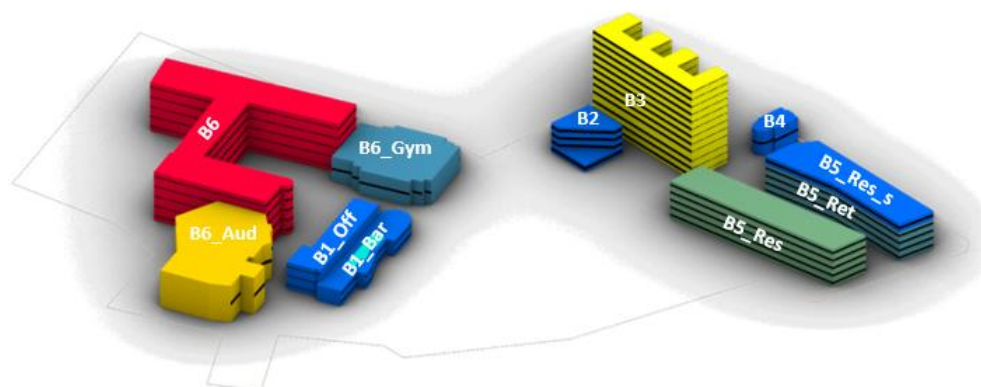


Figure 8. Building energy signature simulation climate 2024 (red for the highest energy demand; blue for the lowest energy demand). B1 = 180 MWh/year; B2 = 87 MWh/year; B3 = 594 MWh/year; B4 = 35 MWh/year; B5 = 646 MWh/year; B6 = 2173 MWh/year.

3.2. EnergyPLAN + MOEA Results

The results of EnergyPLAN + MOEA, in the four types of modeling scenarios, with the two time steps corresponding to 2024 and 2050, are reported, showing the Pareto fronts composed by the optimal solutions, describing them in terms of the composition mix of sustainable energy technologies.

3.2.1. EnergyPLAN + MOEA 2024–2050: “S1: All Sectors and EC Incentive”

Considering the S1 boundaries for the EnergyPLAN + MOEA simulation, the results of Figure 9 are obtained in 2024.

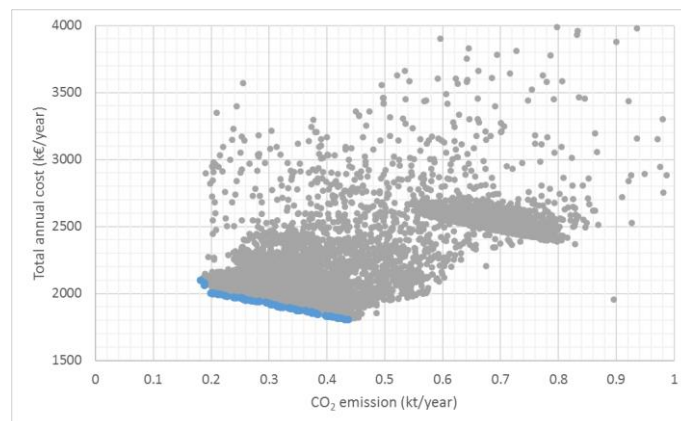


Figure 9. Pareto front of scenario S1 in 2024.

The Pareto front, which represents the 100 optimized solutions, ranges between 0.44 kt/year and 0.18 kt/year, for what concerns CO₂ emission, and between 1806 thousand EUR/year and 2097 thousand EUR/year, for what concerns the total annual cost.

Some important aspects can be noted:

- For values higher than 0.44 kt/year, the algorithm does not identify a contradiction between CO₂ emission reduction and the total annual cost reduction, this means that it is possible to decarbonize and reduce costs at the same time (no conflicting objectives). This point (0.44 kt/year) represents the less costly scenario for the Santa Chiara district.
- EnergyPLAN + MOEA is not able to find solutions for the complete decarbonization of the Santa Chiara district due to a lack of RES both at the district level (limited roof surface to install solar systems) and at the external grid level (electrical import is characterized in 2024 by a partial use of RES).
- From the point 0.44 kt/year (1806 thousand EUR/year), the slope of the Pareto front is more or less constant until the very final part, with CO₂ emissions at 0.2 kt/year (2005 thousand EUR/year), where there is an increase in the slope due to the introduction of more costly decarbonization solutions; in the first part, there is a large reduction of 55% of CO₂ emissions with a modest increase of 11% of the total annual cost (the slope is 829 thousand EUR/kt).

In S1 2024, the decarbonization of the heating sector (Figure 10) is obtained through the large use of heat pumps (1.95–2.12 GWh/year) that are combined with a small amount of natural gas boilers (0.17–0 GWh/year). An important advantage for the heat pumps is that the same capacity, in different time-frames, can be used for both heating and cooling. Solar thermal and H₂ boilers are not considered as attractive decarbonization solutions. Moreover, the decarbonization of the heating sector is already almost complete at the rightmost point of the Pareto front, suggesting that there is almost no contradiction between reducing CO₂ emissions and the total annual cost. This contradiction is only visible in the last part of the Pareto front, with the last two scenarios over 0.2 kt/year, where to completely abandon the natural gas boilers to further reduce CO₂ emissions means increasing the total annual cost. Overall, this is the most convenient and the most highly prioritized sector in which to intervene.

The transport sector (Figure 11) is crucial to further reduce CO₂ emissions. This occurs with a progressive replacement of ICEVs with BEVs starting from 0.44 kt/year where the two types of cars are divided almost equally. This replacement shows a linearity as CO₂ emissions decreases, with a constant slope, as it is also constant in the increase in the total annual cost on the Pareto front. The full replacement of ICEVs with BEVs is completed at 0.2 kt/year.

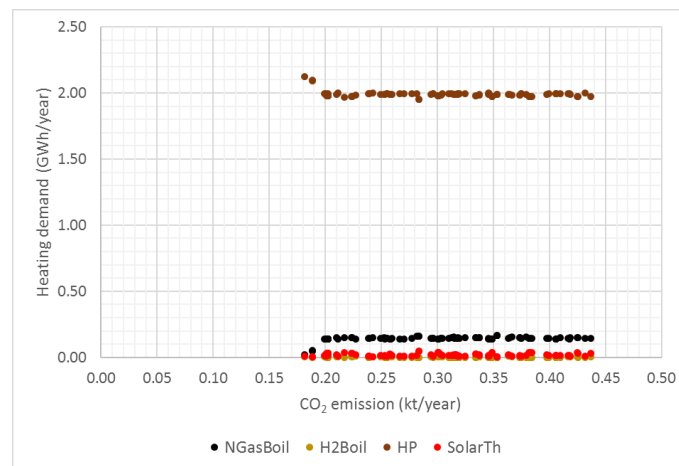


Figure 10. Heating sector of scenario S1 in 2024. The abbreviations used are as follows: Boil = boiler; HP = heat pump; SolarTh = solar thermal.

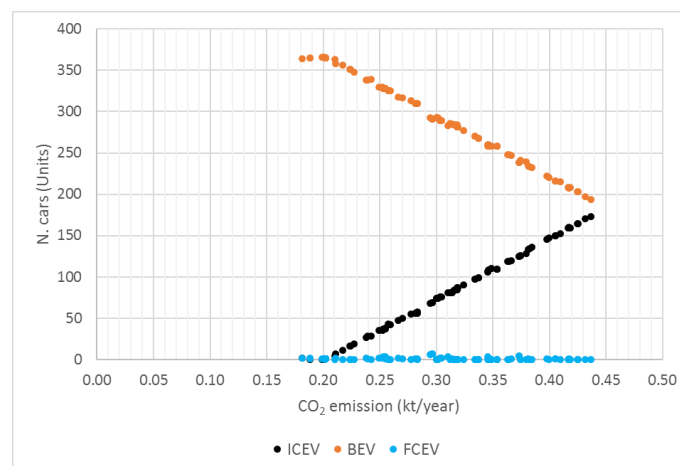


Figure 11. Transport sector of scenario S1 in 2024. The abbreviations used are as follows: ICEV = Internal Combustion Engine Vehicle; BEV = Battery Electric Vehicle; FCEV = Fuel Cell Electric Vehicle.

The electric sector (Figure 12) is characterized by three solutions: PV, import, and export. PV is always maximized and provides 0.8–1.0 GWh/year at all CO₂ emissions, while to satisfy the higher demand by BEV, export is in slight decline (from 0.17 to 0.08 GWh/year) and import is in a stronger increase (from 1.45 to 1.79 GWh/year) along the Pareto front.

The use of electric storage solutions (in the form of batteries or P2P) is not seen as attractive in reducing CO₂ emissions. In fact, all the local electricity production from PV is completely consumed directly by electricity demand or sector coupling with HP and BEV. Towards the left, the Pareto front ends with a full presence of HP in the thermal sector and of BEV in the transport sector, powered by local PV and electric import; exports are practically absent and there is no further way to reduce CO₂ emissions either with the increase in PV (due to space limitations) or with the increase in imports (due to production mix constraints in the regional–national network). Finally, along the Pareto front, the results show that it is necessary to strengthen electricity exchanges with the external grid (see Figure 13) to support the increase in imports, moving from around 780 kW of peak to around 890 kW of peak (+14%).

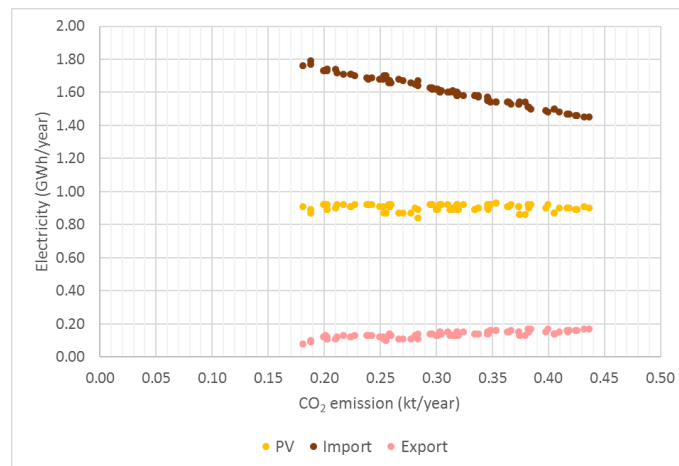


Figure 12. Electricity sector of scenario S1 in 2024.

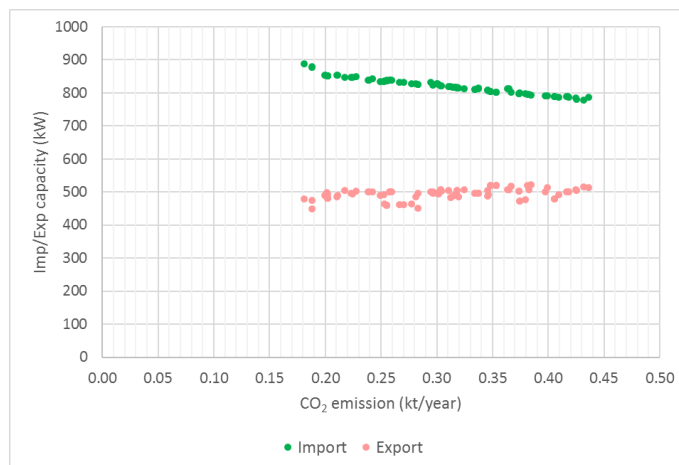


Figure 13. Electricity exchanges with the external grid in S1 2024.

Considering the S1 boundaries for the EnergyPLAN + MOEA simulation, the results of Figure 14 and Supplementary Material D are obtained in 2050 under the assumption of the ERY_h^I climate.

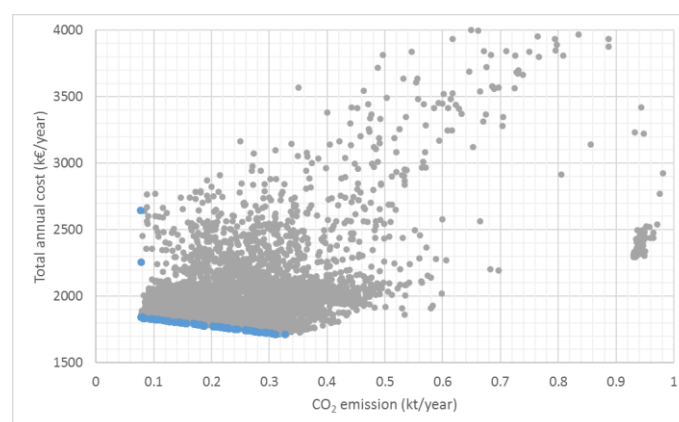


Figure 14. Pareto front of scenario S1 in 2050 ERY_h^I .

In the comparison with the S1 2024 scenario, the following features are highlighted:

- The Pareto front is lower, more to the left, and less steep (524 thousand EUR/kt) because by 2050, the key technologies for the energy transition (PV, HP, and BEV)

are cheaper and more efficient (see Supplementary Material A), and there are other favorable factors such as less heating demand and higher RES share in electricity imports (see Supplementary Material A).

- In the heating sector, decarbonization takes place only through heat pumps; this is thanks to the lower demand for heating, cheaper/more efficient HP (see Supplementary Material A), better combination with cooling, greater production of local PV, and higher RES share in less costly electricity imports (see Supplementary Material A).
- In the transport sector, the full replacement of ICEVs with BEVs is confirmed but more shifted to the left due to cheaper/more efficient BEVs (see Supplementary Material A), greater production of local PV, and a higher RES share in less costly electricity imports.
- In the electricity sector, the behavior is similar but with more local PV production (maximized), less electricity import, and more electricity export; the use of electric storage solutions (in the form of batteries or P2P) is not seen as attractive in reducing CO₂ emissions.

Regarding the S1 boundaries for the EnergyPLAN + MOEA simulation, the results of Supplementary Material D are obtained in 2050 under the assumption of an unchanged climate. Compared to the S1 2024 scenario, the Pareto front is lower, more to the left, and less steep for the same reasons as the scenario S1 in 2050 ERY_h^I . However, the technological choices in the heating, transport, and electricity sectors are practically the same as in the S1 2024 scenario.

3.2.2. EnergyPLAN + MOEA 2024–2050: “S2: All Sectors and NO EC Incentive”

The S2 scenarios consider the absence of the EC incentive. The results of Figure 15 and Supplementary Material D are obtained in 2024.

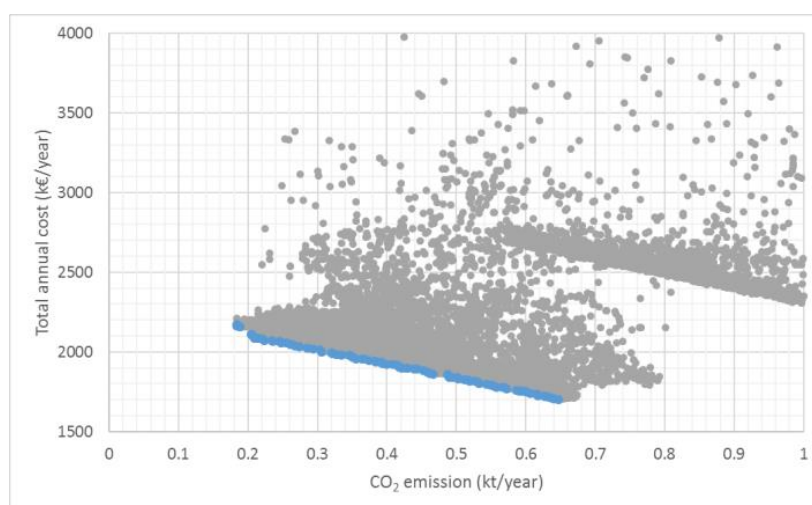


Figure 15. Pareto front of scenario S2 2024.

In the comparison with the S1 2024 scenario, the following features are highlighted:

- The Pareto front is very similar although slightly more steep (868 thousand EUR/kt), higher, and longer on the right due to the absence of the EC incentive.
- The absence of the EC incentive also determines a lower attractiveness for the PV which is not always maximized clearly as in S1 2024 but is sometimes partially preferred to a greater import and a lower export.
- The other technological choices in the heating, transport, and electricity sectors are practically the same as in the S1 2024 scenario.

Moving to the S2 2050 scenarios (see the results in Supplementary Material D), for both ERY_h^I and the unchanged climate, the technological choices in the heating, transport, and electricity sectors are practically the same as in the S1 2050 scenarios, confirming, as

for 2024, the impact of the EC incentive absence on the shape of the Pareto front and on the PV attractiveness.

3.2.3. EnergyPLAN + MOEA 2024–2050: “S3: NO Transport and EC Incentive”

The S3 scenarios consider the absence of the transport sector. The results of Figure 16 and Supplementary Material D are obtained in 2024.

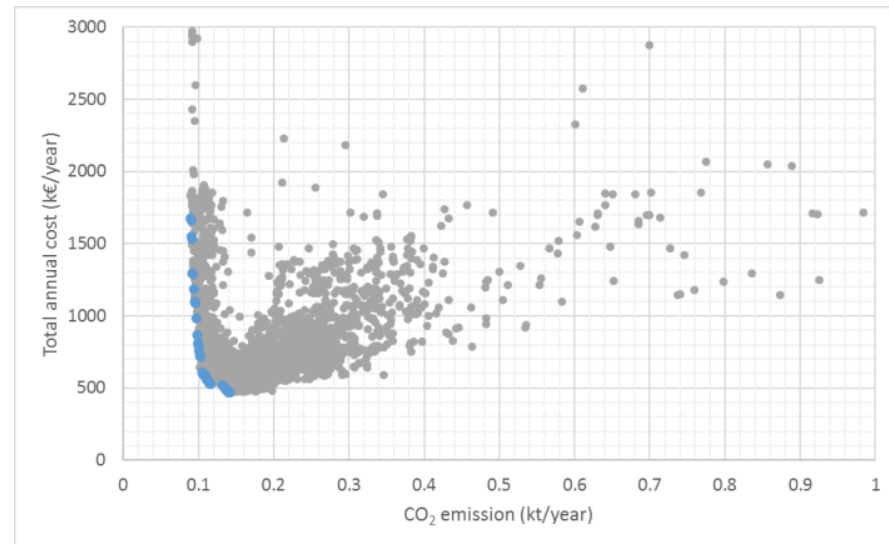


Figure 16. Pareto front of scenario S3 2024.

In the comparison with the S1 2024 scenario, the following features are highlighted:

- The Pareto front is much lower and to the left because it does not include the transport sector; the shape is very different from subvertical to vertical and moving from the point 0.14 kt/year (470 thousand EUR/year) to the point 0.09 kt/year (1675 thousand EUR/year), there is a small reduction of 36% of CO₂ emissions with a large increase of 256% of the total annual cost (the slope is 24100 thousand EUR/kt).
- In the heating sector, decarbonization takes place through heat pumps that only in the first part are combined with a small amount of natural gas boilers.
- In the electricity sector, there is a significant difference due to the increasing integration of batteries to store local PV production (always maximized) and reduce electricity imports (composed of a mix of RES and non-RES): this is a technological approach which implies energy losses in the charge and discharge cycle and above all is very expensive (due to high CAPEX), determining the vertical shape of the Pareto front. Along the Pareto front, the use of batteries is in the range of 0–0.22 GWh/year (of charging). To reach the point of 0.09 kt/year, it is necessary to install a battery system of about 900 kWh in capacity and 450 kW in peak power.

Moving to the S3 2050 scenarios (see the results in Supplementary Material D, Figures 17 and 18), for both ERY_h^I and the unchanged climate, the following features are observed:

- The Pareto front is more to the left because by 2050, the key technologies for the energy transition (PV and HP) are cheaper and more efficient, and there are other favorable factors such as less heating demand and higher RES share in electricity imports.
- The technological choices in the heating and electricity sectors are practically the same as in the S3 2024 scenario, confirming the impact of heat pumps and batteries on the shape of the Pareto front.

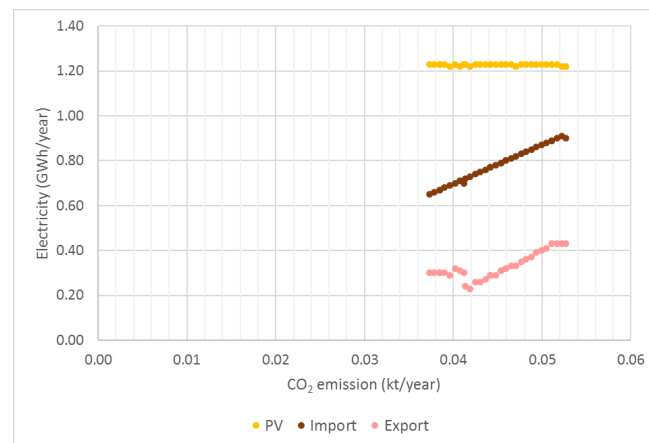


Figure 17. Electricity sector of scenario S3 in 2050 ERY_h^I .

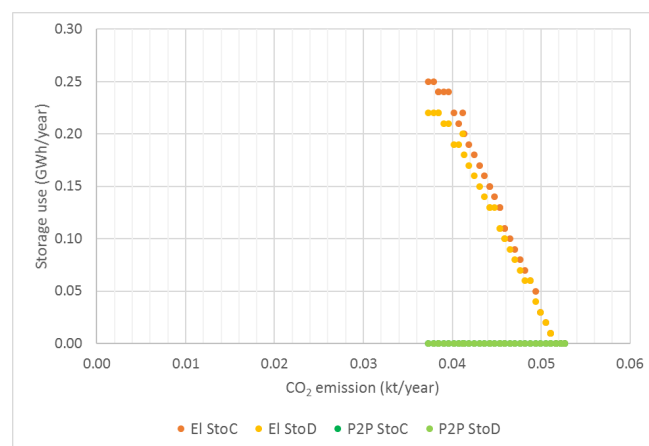


Figure 18. Electricity and P2P storage use in S3 2050 ERY_h^I . The abbreviations used are as follows: El StoC = Electricity Storage Charge (battery charge); El StoD = Electricity Storage Discharge (battery discharge); P2P StoC = Power to Power Storage Charge (P2P Hydrogen Electrolyser); P2P StoD = Power to Power Storage Discharge (P2P Hydrogen Fuel Cell).

3.2.4. EnergyPLAN + MOEA 2024–2050: “S4: Hydrogen vs. Fossil Fuels and EC Incentive”

The last type of scenario considered is S4 characterized by the comparison between hydrogen and fossil fuels. Hydrogen is the only available source for the decarbonization of the heating and transport sectors and only hydrogen P2P systems are considered for electricity storage. The results of Figure 19 and Supplementary Material D are obtained in 2024.

In the comparison with the S1 2024 scenario, the following features are highlighted:

- The Pareto front is higher, to the right, and steeper because this energy transition based only on hydrogen technologies is more costly, less efficient, and with a lower capability to reach high decarbonization based on the limited local RES in the district.
- Two sections with different slopes can be distinguished; from the point 1.03 kt/year (1731 thousand EUR/year), the slope of the Pareto front is more or less constant (2720 thousand EUR/kt) until the CO₂ emissions of 0.54 kt/year (3064 thousand EUR/year) where the second part starts with an increased slope (13,225 thousand EUR/kt) due to the introduction of more costly decarbonization solutions (until 0.42 kt/year and 4651 thousand EUR/year).
- In the heating sector (Figure 20), decarbonization takes place through H₂ boilers that in the first part of the Pareto front are limited and combined with a larger amount of natural gas boilers, while in the second part are increasing and overtaking the fossil

fuel solution that, however, does not completely disappear in the leftmost part of the Pareto front (due to a lack of RES both at the district and at external grid levels).

- In the transport sector (Figure 21), the full replacement of ICEVs with FCEVs occurs in the first part of the Pareto front: in this scenario, decarbonization takes place as a priority in the transport sector compared to the thermal sector, and FCEVs are more attractive than H2 boilers, with the exception of the limited quantity of the latter which is present from the far right part of the Pareto front.
- In the electricity sector (Figure 22), in addition to the always maximized PV, three parts can be distinguished: (I) between 1.03 kt/year and 0.84 kt/year, import is constant and export slightly decreasing up to zero, and this strategy is due to the higher electricity demand to produce H2 and request to reduce CO₂ emission; (II) between 0.84 kt/year and 0.54 kt/year, import is increasing rapidly, following the increasing demand of H2 production for FCEV; (III) between 0.54 kt/year and the end of the Pareto front, the slope of the import rise is even stronger due to the quick ascent of H2 boilers.
- The use of P2P as an electric storage solution is not seen as attractive in reducing CO₂ emissions. In fact, all the local electricity production from PV is completely consumed directly by electricity demand or sector coupling with H2 boilers and FCEV, exports are practically nil, and there is no further way to reduce CO₂ emissions either with the increase in PV (due to space limitations) or with the increase in imports (due to production mix constraints in the regional–national network). Finally, along the Pareto front, the results show that it is necessary to strengthen electricity exchanges with the external grid (Figure 23) to support the increase in imports, moving from around 500 kW of peak to an impressive 2260 kW of peak (+452%).

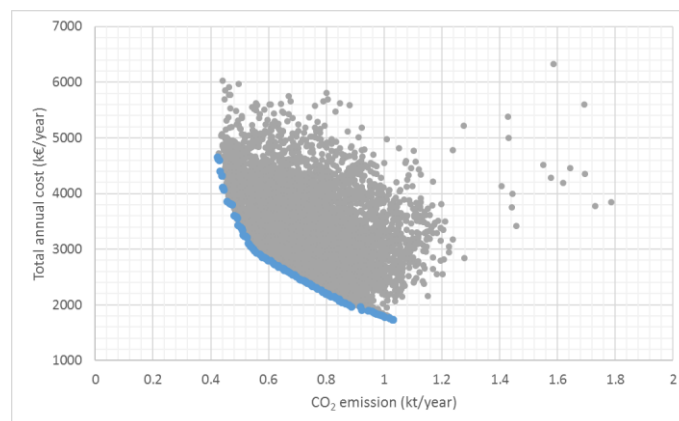


Figure 19. Pareto front of scenario S4 in 2024.

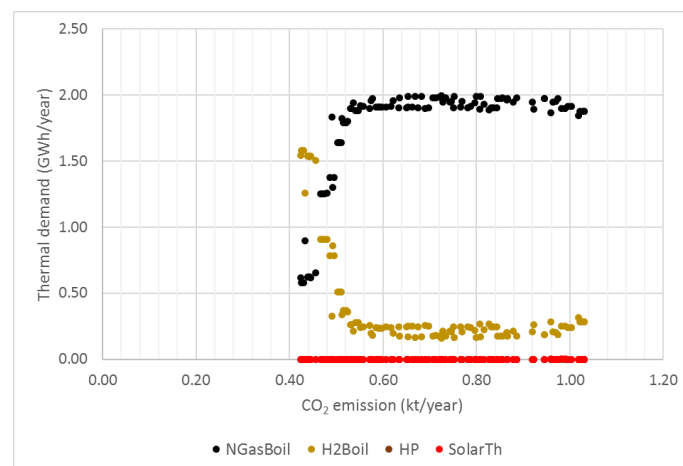


Figure 20. Heating sector of scenario S4 in 2024.

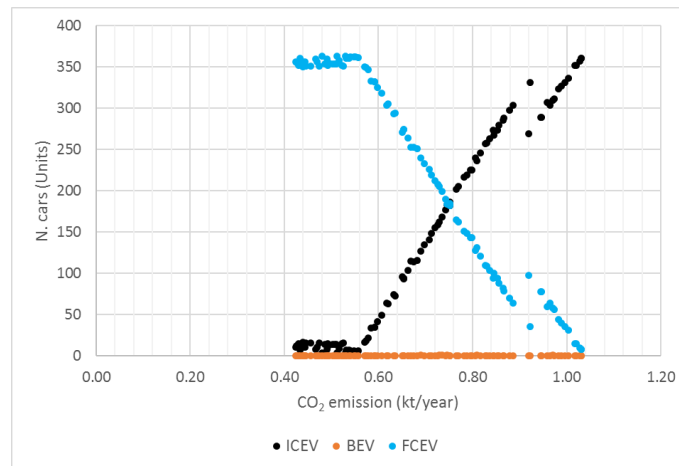


Figure 21. Transport sector of scenario S4 in 2024.

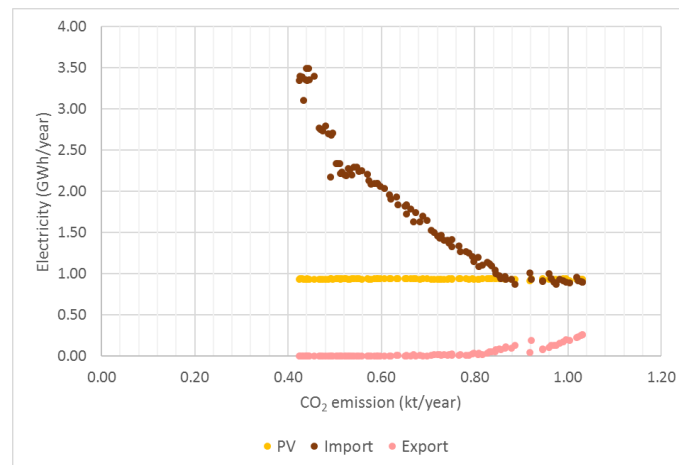


Figure 22. Electricity sector of scenario S4 in 2024.

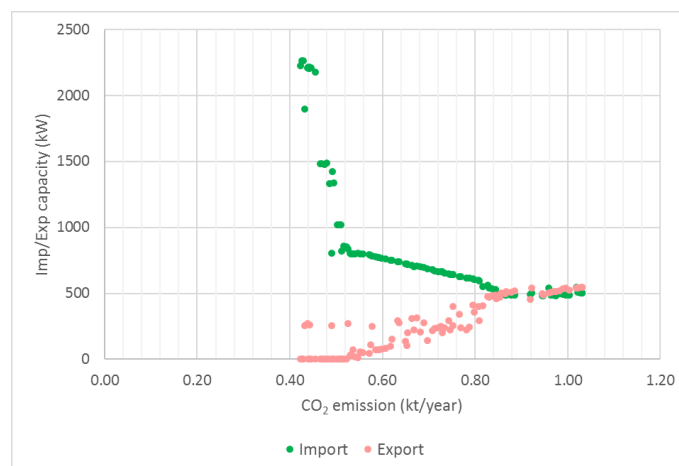


Figure 23. Electricity exchanges with the external grid in S4 2024.

Moving to the S4 2050 scenarios (see the results in Supplementary Material D), for both ERY_h^I and the unchanged climate, the following features are observed:

- The Pareto front is more to the left because by 2050, the key technologies for the energy transition (PV, H2 boilers, and FCEV) are cheaper and more efficient, and there are

other favorable factors such as less heating demand and higher RES share in electricity imports.

- The technological choices in the heating, transport, and electricity sectors are practically the same as in the S4 2024 scenario, confirming the impact of H2 boilers and FCEVs on the shape of the Pareto front.

Finally, Figure 24 well represents and summarizes the comparison between the 12 Pareto fronts discussed in this Results Section. The Reader can see (I) within the same type of scenario the beneficial effects for (an easier) decarbonisation of climate change (e.g., 2024 vs. 2050 ERY_h^I) and of technological improvement (e.g., 2024 vs. 2050 UC and 2050 ERY_h^I), (II) between different scenarios the beneficial effect of EC incentives (e.g., S1 vs S2, even if very limited), and (III) between different scenarios the negative effect of adopting restrictive constraints (e.g., S1 vs. S4, where S4 relies only on hydrogen).

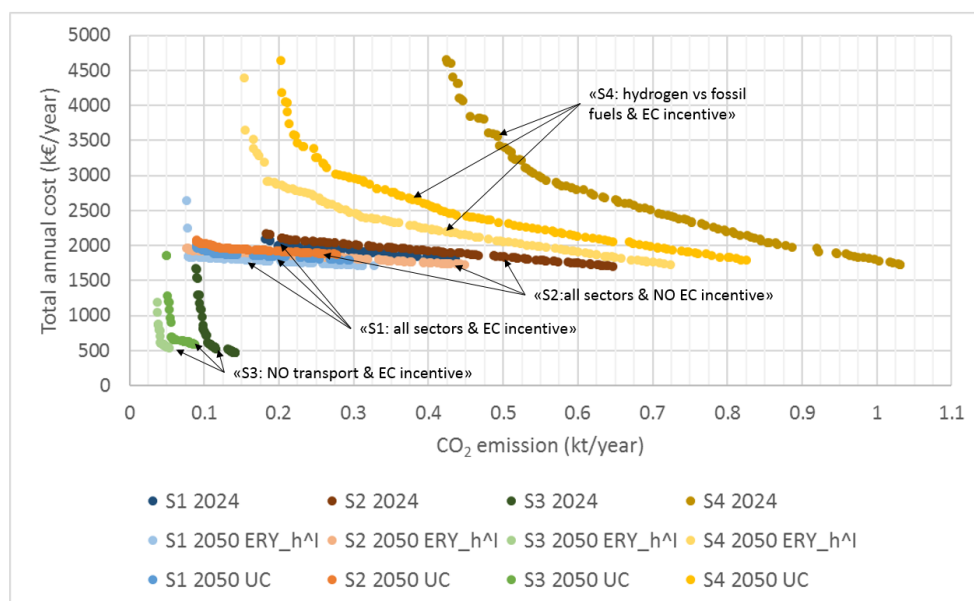


Figure 24. Comparison between Pareto fronts.

4. Conclusions

In this paper, an effort has been carried out for an urban neighborhood of six buildings in Trento (Italy) to design decarbonization energy scenarios for the years 2024 and 2050, also accounting for different climatic conditions for these two time periods.

Firstly, the six buildings are modeled with the Urban Modeling Interface (umi) tool to evaluate the energy performance in 2024 and 2050, computing the dynamic (hourly) energy demands for space heating, domestic hot water, space cooling, and electricity. The district transport demand is also considered based on the parking spaces pertaining to each building and evaluating the annual and hourly demand of energy for the mobility of each parking space. Then, EnergyPLAN coupled with a multi-objective evolutionary algorithm (MOEA) is used to investigate 12 different energy decarbonization scenarios in 2024 and 2050 based on different boundaries for RESs, energy storage, hydrogen, energy system integration, and energy community incentives. Two conflicting objectives are considered: cost and CO₂ emission reductions.

Hence, in each of the 12 scenarios, the EnergyPLAN + MOEA framework is adopted to automatically find the optimal future solutions, leading to the identification of 100 optimal energy systems on the Pareto front out of 10,000 simulated ones in a short computational time of about 5 h. The study tested the capabilities of the optimization algorithms by considering very complex energy systems, including electricity, heating, cooling, transport, several RESs, cross-sector interactions, storage, and hydrogen technologies.

The innovative contribution lies in the integration of EnergyPLAN with both detailed umi modeling and MOEA to find the optimal energy scenarios for an urban neighborhood both in the current (2024) and in the future (2050) climate, considering the PED and energy community approaches. Altogether, these aspects are innovative considering that the usual energy scenario modeling is based on yearly balances, ignores smart sector coupling, and misses proper optimization. Different policy/investment visions are formulated as the boundary variables for decision making, and this approach opens up a very large number of possibilities for local policy makers/investors.

Considering S1 with all sectors and EC incentive, the results show that by 2024, EnergyPLAN + MOEA is not able to find solutions for the complete decarbonization of the Santa Chiara district (minimum value is 0.18 kt/year) due to a lack of RES both at the district level (limited roof surface to install solar systems) and at the external grid level (electrical import is characterized in 2024 by partial use of RES). Moreover, in 2024, the decarbonization of the heating sector is prioritized and obtained through the large use of reversible heat pumps (1.95–2.12 GWh/year) that are combined with a small amount of natural gas boilers (0.17–0 GWh/year). Solar thermal (sharing the same roof surface as PV) and H₂ boilers are not considered as attractive decarbonization solutions. The transport sector is crucial to further reduce CO₂ emission, and this occurs with a progressive replacement of ICEVs with BEVs (the full replacement of ICEVs with BEVs is completed at 0.2 kt/year). Supporting these electrification technologies, PV is always maximized (0.8–1.0 GWh/year) while export is in slight decline (from 0.17 to 0.08 GWh/year) and import is in a stronger increase (from 1.45 to 1.79 GWh/year) along the Pareto front. The use of electric storage is not seen as attractive in reducing CO₂ emissions. By 2050, in comparison to the climate model 2024, for the same CO₂ emissions, the total annual costs are lower and the Pareto front is less steep (e.g., 829 thousand EUR/kt in 2024 and 524 thousand EUR/kt in 2050 ERY_h^I) because the key technologies for the energy transition (PV, HP, and BEV) are cheaper and more efficient, and there are other favorable factors such as less heating demand and higher RES share in electricity imports (same as in the other types of 2050 scenarios).

The absence of an EC incentive, as explored in S2, results in a slightly “less attractive” Pareto front (868 thousand EUR/kt in 2024), reducing the local PV attractiveness. Interesting is S3 where the transport sector is removed from the modeling to focus only on the thermal (heating and cooling) and electrical sectors. This approach confirms not only the priority choice of heat pumps but also that the integration of batteries is unattractive in the context of the Santa Chiara district: it implies energy losses in the charge and discharge cycle and above all is very expensive (due to high CAPEX), determining the vertical shape of the Pareto front (24,100 thousand EUR/kt in 2024). Moreover, clear results are also explored in S4 characterized by the comparison between hydrogen and fossil fuels: for the same CO₂ emissions of S1, the total annual costs are higher and the Pareto front is steeper (from 2720 thousand EUR/kt to 13225 thousand EUR/kt in 2024) because this energy transition, based only on hydrogen technologies (i.e., H₂ boilers and FCEV), is more costly, less efficient, and with a lower capability to reach high decarbonization (minimum value is 0.42 kt/year in 2024) based on the limited local RESs in the district.

Overall, this study confirms the important role of the energy system integration approach: the interconnection of the sectors allows optimizing the energy system as a whole with greater economic efficiency than decarbonizing and improving the efficiency of each sector separately. Moreover, policy makers and investors can see, from one side, the beneficial effects of modeling/considering climate change, technological improvements, and EC incentives and from the other side, the negative effects of adopting restrictive constraints (e.g., relying only on hydrogen for the energy transition).

Supplementary Materials: The following supporting information can be downloaded at: <https://www.mdpi.com/article/10.3390/en17164047/s1>, Supplementary Material A: Input data for the use of EnergyPLAN in the Santa Chiara district case study; Supplementary Material B: MOEA boundaries in the four types of simulation scenarios; Supplementary Material C: Extra formulas (additional algorithms for model adjustment); Supplementary Material D: Santa Chiara district energy system: results of the EnergyPLAN+MOEA scenarios in S1 2050 ERY_h^I , S1 2050 UC, S2 2024, S2 2050 ERY_h^I , S2 2050 UC, S3 2024, S3 2050 ERY_h^I , S3 2050 UC, S4 2024, S4 2050 ERY_h^I , S4 2050 UC.

Author Contributions: Conceptualization, D.V., G.P. and M.S.M.; methodology, D.V., G.P. and M.S.M.; software, G.B. and M.S.M.; validation, D.V. and G.P.; formal analysis, G.B. and S.R.; investigation, G.B. and S.R.; resources, G.B. and S.R.; data curation, D.V., G.B. and S.R.; writing—original draft preparation, D.V.; writing—review and editing, D.V., G.B. and G.P.; visualization, D.V., G.B. and G.P.; supervision, D.V. and G.P.; project administration, D.V. and G.P.; funding acquisition, D.V. and G.P. All authors have read and agreed to the published version of the manuscript.

Funding: The research leading to these results has received funding from the European Union’s Horizon Europe research and innovation program under the project InCUBE, grant agreement No 101069610. The authors would like to acknowledge the European Commission for the support granted to InCUBE. The authors are grateful to the Municipality of Trento and Habitat S.p.a. for the support during the activities within the “Demo Trento—Santa Chiara District”, including data provision. A part of this manuscript has been completed in the framework of the PhD Research Scholarship “Development of urban building energy models to support the definition of energy policies by municipalities and local public administrations” (DM 118/2023). Finally, the authors would like to thank all the anonymous reviewers for their valuable comments and suggestions to improve the article.

Data Availability Statement: Data are available upon request.

Conflicts of Interest: The authors declare no conflicts of interest.

References

1. United Nations. Kyoto Protocol to the United Nations Framework Convention on Climate Change. 1998. Available online: https://unfccc.int/kyoto_protocol (accessed on 17 June 2024).
2. United Nations. Paris Agreement. 2015. Available online: <https://unfccc.int/process-and-meetings/the-paris-agreement> (accessed on 17 June 2024).
3. European Commission. The European Green Deal. 2019. Available online: https://commission.europa.eu/strategy-and-policy/priorities-2019-2024/european-green-deal_en (accessed on 17 June 2024).
4. European Commission. Renovation Wave Strategy. 2020. Available online: https://ec.europa.eu/commission/presscorner/detail/en/ip_20_1835 (accessed on 17 June 2024).
5. Available online: <https://jpi-urbaneurope.eu/ped/> (accessed on 17 May 2024).
6. Bossi, S.; Gollner, C.; Theierling, S. Towards 100 positive energy districts in Europe: Preliminary data analysis of 61 European cases. *Energies* **2020**, *13*, 6083. [[CrossRef](#)]
7. JPI Urban Europe. Europe towards Positive Energy Districts. 2020. Available online: https://jpi-urbaneurope.eu/wp-content/uploads/2020/06/PED-Booklet-Update-Feb-2020_2.pdf (accessed on 17 June 2024).
8. Available online: <https://incubeproject.eu/> (accessed on 17 May 2024).
9. Buckley, N.; Mills, G.; Reinhart, C.; Berzolla, Z.M. Using urban building energy modelling (UBEM) to support the new European Union’s Green Deal: Case study of Dublin Ireland. *Energy Build.* **2021**, *247*, 111115. [[CrossRef](#)]
10. Perwez, U.; Shono, K.; Yamaguchi, Y.; Shimoda, Y. Multi-scale UBEM-BIPV coupled approach for the assessment of carbon neutrality of commercial building stock. *Energy Build.* **2023**, *291*, 113086. [[CrossRef](#)]
11. Battini, F.; Pernigotto, G.; Gasparella, A. District-level validation of a shoeboxing simplification algorithm to speed-up Urban Building Energy Modeling simulations. *Appl. Energy* **2023**, *349*, 121570. [[CrossRef](#)]
12. Dogan, T.; Reinhart, C. Automated Conversion of Architectural Massing Models into Thermal ‘Shoebox’ Models. In Proceedings of the 13th Conference of International Building Performance Simulation Association, Chambéry, France, 26–28 August 2013. [[CrossRef](#)]
13. Lund, H.; Thellufsen, J.Z.; Østergaard, P.A.; Sorknæs, P.; Skov, I.R.; Mathiesen, B.V. Energy PLAN—Advanced analysis of smart energy systems. *Smart Energy* **2021**, *1*, 100007. [[CrossRef](#)]
14. Lund, H.; Andersen, A.N.; Østergaard, P.A.; Mathiesen, B.V.; Connolly, D. From electricity smart grids to smart energy systems—a market operation based approach and understanding. *Energy* **2012**, *42*, 96–102. [[CrossRef](#)]

15. Lund, H.; Østergaard, P.A.; Connolly, D.; Mathiesen, B.V. Smart energy and smart energy systems. *Energy* **2017**, *137*, 556–565. [[CrossRef](#)]
16. Mathiesen, B.V.; Lund, H.; Connolly, D.; Wenzel, H.; Østergaard, P.A.; Möller, B.; Nielsen, S.; Ridjan, I.; Karnøe, P.; Sperling, K.; et al. Smart Energy Systems for coherent 100% renewable energy and transport solutions. *Appl. Energy* **2015**, *145*, 139–154. [[CrossRef](#)]
17. Bhuvanesh, A.; Christa, S.J.; Kannan, S.; Pandiyan, M.K. Aiming towards pollution free future by high penetration of renewable energy sources in electricity generation expansion planning. *Futures* **2018**, *104*, 25–36. [[CrossRef](#)]
18. Cantarero, M.M.V. Reviewing the Nicaraguan transition to a renewable energy system: Why is “business-as-usual” no longer an option? *Energy Policy* **2018**, *120*, 580–592. [[CrossRef](#)]
19. Kiwan, S.; Al-Gharibeh, E. Jordan toward a 100% renewable electricity system. *Renew. Energy* **2020**, *147*, 423–436. [[CrossRef](#)]
20. Matak, N.; Tomić, T.; Schneider, D.R.; Krajačić, G. Integration of WtE and district cooling in existing Gas-CHP based district heating system—Central European city perspective. *Smart Energy* **2021**, *4*, 100043. [[CrossRef](#)]
21. Campos, J.; Csontos, C.; Munkácsy, B. Electricity scenarios for Hungary: Possible role of wind and solar resources in the energy transition. *Energy* **2023**, *278*, 127971. [[CrossRef](#)]
22. Dominković, D.F.; Rashid, K.B.A.; Romagnoli, A.; Pedersen, A.S.; Leong, K.C.; Krajačić, G.; Duić, N. Potential of district cooling in hot and humid climates. *Appl. Energy* **2017**, *208*, 49–61. [[CrossRef](#)]
23. Bamisile, O.; Obiora, S.; Huang, Q.; Okonkwo, E.C.; Olagoke, O.; Shokanbi, A.; Kumar, R. Towards a sustainable and cleaner environment in China: Dynamic analysis of vehicle-to-grid, batteries and hydro storage for optimal RE integration. *Sustain. Energy Technol. Assess.* **2020**, *42*, 100872. [[CrossRef](#)]
24. Bamisile, O.; Babatunde, A.; Adun, H.; Yimen, N.; Mukhtar, M.; Huang, Q.; Hu, W. Electrification and renewable energy nexus in developing countries; an overarching analysis of hydrogen production and electric vehicles integrality in renewable energy penetration. *Energy Convers. Manag.* **2021**, *236*, 114023. [[CrossRef](#)]
25. Doepfert, M.; Castro, R. Techno-economic optimization of a 100% renewable energy system in 2050 for countries with high shares of hydropower: The case of Portugal. *Renew. Energy* **2021**, *165*, 491–503. [[CrossRef](#)]
26. Tomić, T.; Dominković, D.F.; Pfeifer, A.; Schneider, D.R.; Pedersen, A.S.; Duić, N. Waste to energy plant operation under the influence of market and legislation conditioned changes. *Energy* **2017**, *137*, 1119–1129. [[CrossRef](#)]
27. Pupo-Roncallo, O.; Campillo, J.; Ingham, D.; Ma, L.; Pourkashanian, M. The role of energy storage and cross-border interconnections for increasing the flexibility of future power systems: The case of Colombia. *Smart Energy* **2021**, *2*, 100016. [[CrossRef](#)]
28. Pastore, L.M.; Basso, G.L.; Cristiani, L.; de Santoli, L. Rising targets to 55% GHG emissions reduction—The smart energy systems approach for improving the Italian energy strategy. *Energy* **2022**, *259*, 125049. [[CrossRef](#)]
29. Cabrera, P.; Lund, H.; Thellufsen, J.Z.; Sorknaes, P. The MATLAB Toolbox for EnergyPLAN: A tool to extend energy planning studies. *Sci. Comput. Program.* **2020**, *191*, 102405. [[CrossRef](#)]
30. De Luca, G.; Fabozzi, S.; Massarotti, N.; Vanoli, L. A renewable energy system for a nearly zero greenhouse city: Case study of a small city in southern Italy. *Energy* **2018**, *143*, 347–362. [[CrossRef](#)]
31. Bonati, A.; De Luca, G.; Fabozzi, S.; Massarotti, N.; Vanoli, L. The integration of exergy criterion in energy planning analysis for 100% renewable system. *Energy* **2019**, *174*, 749–767. [[CrossRef](#)]
32. Calise, F.; Fabozzi, S.; Vanoli, L.; Vicidomini, M. A sustainable mobility strategy based on electric vehicles and photovoltaic panels for shopping centers. *Sustain. Cities Soc.* **2021**, *70*, 102891. [[CrossRef](#)]
33. Battaglia, V.; De Luca, G.; Fabozzi, S.; Lund, H.; Vanoli, L. Integrated energy planning to meet 2050 European targets: A Southern Italian region case study. *Energy Strategy Rev.* **2022**, *41*, 100844. [[CrossRef](#)]
34. Novosel, T.; Perković, L.; Ban, M.; Keko, H.; Pukšec, T.; Krajačić, G.; Duić, N. Agent based modelling and energy planning—Utilization of MATSim for transport energy demand modelling. *Energy* **2015**, *92*, 466–475. [[CrossRef](#)]
35. Thellufsen, J.Z.; Nielsen, S.; Lund, H. Implementing cleaner heating solutions towards a future low-carbon scenario in Ireland. *J. Clean. Prod.* **2019**, *214*, 377–388. [[CrossRef](#)]
36. Groppi, D.; Garcia, D.A.; Basso, G.L.; De Santoli, L. Synergy between smart energy systems simulation tools for greening small Mediterranean islands. *Renew. Energy* **2019**, *135*, 515–524. [[CrossRef](#)]
37. Østergaard, P.A.; Jantzen, J.; Marcinkowski, H.M.; Kristensen, M. Business and socioeconomic assessment of introducing heat pumps with heat storage in small-scale district heating systems. *Renew. Energy* **2019**, *139*, 904–914. [[CrossRef](#)]
38. Pfeifer, A.; Dobravec, V.; Pavlinek, L.; Krajačić, G.; Duić, N. Integration of renewable energy and demand response technologies in interconnected energy systems. *Energy* **2018**, *161*, 447–455. [[CrossRef](#)]
39. Bačeković, I.; Østergaard, P.A. Local smart energy systems and cross-system integration. *Energy* **2018**, *151*, 812–825. [[CrossRef](#)]
40. Lund, R.; Ilic, D.D.; Trygg, L. Socioeconomic potential for introducing large-scale heat pumps in district heating in Denmark. *J. Clean. Prod.* **2016**, *139*, 219–229. [[CrossRef](#)]
41. Pillai, J.R.; Heussen, K.; Østergaard, P.A. Comparative analysis of hourly and dynamic power balancing models for validating future energy scenarios. *Energy* **2011**, *36*, 3233–3243. [[CrossRef](#)]
42. Jiménez, A.; Cabrera, P.; Medina, J.F.; Østergaard, P.A.; Lund, H. Smart energy system approach validated by electrical analysis for electric vehicle integration in islands. *Energy Convers. Manag.* **2024**, *302*, 118121. [[CrossRef](#)]

43. Olkkonen, V.; Rinne, S.; Hast, A.; Syri, S. Benefits of DSM measures in the future Finnish energy system. *Energy* **2017**, *137*, 729–738. [[CrossRef](#)]
44. Mahbub, M.S.; Cozzini, M.; Østergaard, P.A.; Alberti, F. Combining multi-objective evolutionary algorithms and descriptive analytical modelling in energy scenario design. *Appl. Energy* **2016**, *164*, 140–151. [[CrossRef](#)]
45. Prina, M.G.; Fanali, L.; Manzolini, G.; Moser, D.; Sparber, W. Incorporating combined cycle gas turbine flexibility constraints and additional costs into the EPLANopt model: The Italian case study. *Energy* **2018**, *160*, 33–43. [[CrossRef](#)]
46. Bellocchi, S.; Manno, M.; Noussan, M.; Prina, M.G.; Vellini, M. Electrification of transport and residential heating sectors in support of renewable penetration: Scenarios for the Italian energy system. *Energy* **2020**, *196*, 117062. [[CrossRef](#)]
47. Herc, L.; Pfeifer, A.; Duić, N. Optimization of the possible pathways for gradual energy system decarbonization. *Renew. Energy* **2022**, *193*, 617–633. [[CrossRef](#)]
48. Laha, P.; Chakraborty, B. Low carbon electricity system for India in 2030 based on multi-objective multi-criteria assessment. *Renew. Sustain. Energy Rev.* **2021**, *135*, 110356. [[CrossRef](#)]
49. Viesi, D.; Crema, L.; Mahbub, M.S.; Veronesi, S.; Brunelli, R.; Baggio, P.; Fauri, M.; Prada, A.; Bello, A.; Nodari, B.; et al. Integrated and dynamic energy modelling of a regional system: A cost-optimized approach in the deep decarbonisation of the Province of Trento (Italy). *Energy* **2020**, *209*, 118378. [[CrossRef](#)]
50. Bellocchi, S.; Guidi, G.; De Iulio, R.; Manno, M.; Nastasi, B.; Noussan, M.; Prina, M.G.; Roberto, R. Analysis of smart energy system approach in local alpine regions—A case study in Northern Italy. *Energy* **2020**, *202*, 117748. [[CrossRef](#)]
51. Prina, M.G.; Cozzini, M.; Garegnani, G.; Manzolini, G.; Moser, D.; Oberegger, U.F.; Perneti, R.; Vaccaro, R.; Sparber, W. Multi-objective optimization algorithm coupled to EnergyPLAN software: The EPLANopt model. *Energy* **2018**, *149*, 213–221. [[CrossRef](#)]
52. Vaccaro, R.; Rocco, M.V. Quantifying the impact of low carbon transition scenarios at regional level through soft-linked energy and economy models: The case of South-Tyrol Province in Italy. *Energy* **2021**, *220*, 119742. [[CrossRef](#)]
53. Prina, M.G.; Moser, D.; Vaccaro, R.; Sparber, W. EPLANopt optimization model based on EnergyPLAN applied at regional level: The future competition on excess electricity production from renewables. *Int. J. Sustain. Energy Plan. Manag.* **2020**, *27*, 35–50. [[CrossRef](#)]
54. Mahbub, M.S.; Viesi, D.; Cattani, S.; Crema, L. An innovative multi-objective optimization approach for long-term energy planning. *Appl. Energy* **2017**, *208*, 1487–1504. [[CrossRef](#)]
55. Mahbub, M.S.; Viesi, D.; Crema, L. Designing optimized energy scenarios for an Italian Alpine valley: The case of Giudicarie Esteriori. *Energy* **2016**, *116*, 236–249. [[CrossRef](#)]
56. Cabrera, P.; Carta, J.A.; Lund, H.; Thellufsen, J.Z. Large-scale optimal integration of wind and solar photovoltaic power in water-energy systems on islands. *Energy Convers. Manag.* **2021**, *235*, 113982. [[CrossRef](#)]
57. Groppi, D.; Nastasi, B.; Prina, M.G.; Garcia, D.A. The EPLANopt model for Favignana island’s energy transition. *Energy Convers. Manag.* **2021**, *241*, 114295. [[CrossRef](#)]
58. Yuan, M.; Thellufsen, J.Z.; Sorknæs, P.; Lund, H.; Liang, Y. District heating in 100% renewable energy systems: Combining industrial excess heat and heat pumps. *Energy Convers. Manag.* **2021**, *244*, 114527. [[CrossRef](#)]
59. Prina, M.G.; Cozzini, M.; Garegnani, G.; Moser, D.; Oberegger, U.F.; Vaccaro, R.; Sparber, W. Smart energy systems applied at urban level: The case of the municipality of Bressanone-Brixen. *Int. J. Sustain. Energy Plan. Manag.* **2016**, *10*, 33–52. [[CrossRef](#)]
60. de Maigret, J.; Viesi, D.; Mahbub, M.S.; Testi, M.; Cuonzo, M.; Thellufsen, J.Z.; Østergaard, P.A.; Lund, H.; Baratieri, M.; Crema, L. A multi-objective optimization approach in defining the decarbonization strategy of a refinery. *Smart Energy* **2022**, *6*, 100076. [[CrossRef](#)]
61. Viesi, D.; Mahbub, M.S.; Brandi, A.; Thellufsen, J.Z.; Østergaard, P.A.; Lund, H.; Baratieri, M.; Crema, L. Multi-objective optimization of an energy community: An integrated and dynamic approach for full decarbonisation in the European Alps. *Int. J. Sustain. Energy Plan. Manag.* **2023**, *38*, 8–29. [[CrossRef](#)]
62. Roman, O.; Farella, E.M.; Rigon, S.; Remondino, F.; Ricciuti, S.; Viesi, D. From 3D surveying data to BIM to BEM: The InCUBE dataset. *Int. Arch. Photogramm. Remote Sens. Spat. Inf. Sci.* **2023**, *48*, 175–182. [[CrossRef](#)]
63. Ziozas, N.; Kitsopoulou, A.; Bellos, E.; Iliadis, P.; Gonidaki, D.; Angelakoglou, K.; Nikolopoulos, N.; Ricciuti, S.; Viesi, D. Energy Performance Analysis of the Renovation Process in an Italian Cultural Heritage Building. *Sustainability* **2024**, *16*, 2784. [[CrossRef](#)]
64. CTI Comitato Termotecnico Italiano—Vendita Documenti Normativi. Available online: <https://try.cti2000.it/> (accessed on 13 November 2023).
65. Pernigotto, G.; Prada, A.; Gasparella, A. Extreme reference years for building energy performance simulation. *J. Build. Perform. Simul.* **2020**, *13*, 152–166. [[CrossRef](#)]
66. Available online: <https://www.ashrae.org/> (accessed on 17 May 2024).
67. U.S. Department of Energy. DOE Commercial Building Energy Asset Score: Software Development for Phase II Building Types. Available online: <https://www.energy.gov/eere/buildings/articles/doe-commercial-building-energy-asset-score-software-development-phase-ii> (accessed on 13 July 2023).
68. U.S. Department of Energy. Prototype Building Models. Available online: <https://www.energycodes.gov/prototype-building-models#IECC> (accessed on 13 July 2023).

69. Available online: <https://store.uni.com/uni-ts-11300-1-2014> (accessed on 17 June 2024).
70. Available online: <https://store.uni.com/uni-10339-1995> (accessed on 17 June 2024).

Disclaimer/Publisher’s Note: The statements, opinions and data contained in all publications are solely those of the individual author(s) and contributor(s) and not of MDPI and/or the editor(s). MDPI and/or the editor(s) disclaim responsibility for any injury to people or property resulting from any ideas, methods, instructions or products referred to in the content.